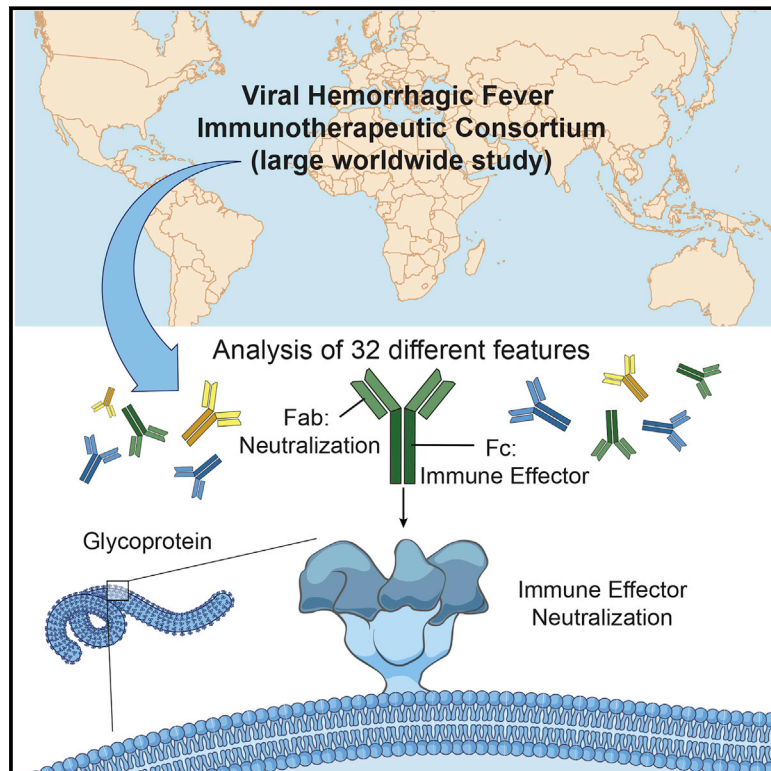


Systematic Analysis of Monoclonal Antibodies against Ebola Virus GP Defines Features that Contribute to Protection

Graphical Abstract



Highlights

- Global collaborative study to define mAb features that protect against Ebola virus
- Single neutralization assays are not always predictive of in vivo mAb efficacy
- Immune effector function can contribute to and may drive mAb-mediated protection
- Protection and neutralization are not influenced by sGP

Authors

Erica Ollmann Saphire, Sharon L. Schendel, Marnie L. Fusco, ..., Kartik Chandran, John M. Dye, the Viral Hemorrhagic Fever Immunotherapeutic Consortium

Correspondence

erica@scripps.edu (E.O.S.), gary.kobinger@crchudequebec.ulaval.ca (G.P.K.), andersen@scripps.edu (K.G.A.), kawaokay@svm.vetmed.wisc.edu (Y.K.), galter@mgh.harvard.edu (G.A.), kartik.chandran@einstein.yu.edu (K.C.), john.m.dye1.civ@mail.mil (J.M.D.)

In Brief

The systematic assessment of the effector functions and binding sites of antibodies against Ebola virus provides a generalizable framework to evaluate the determinants of antibody-mediated protection in viral disease.



Systematic Analysis of Monoclonal Antibodies against Ebola Virus GP Defines Features that Contribute to Protection

Erica Ollmann Saphire,^{1,28,*} Sharon L. Schendel,^{1,27} Marnie L. Fusco,^{1,27} Karthik Gangavarapu,^{1,27} Bronwyn M. Gunn,^{3,27} Anna Z. Wec,^{4,27} Peter J. Halfmann,^{6,27} Jennifer M. Brannan,^{7,27} Andrew S. Herbert,^{7,27} Xiangguo Qiu,^{8,27} Kshitij Wagh,^{9,27} Shihua He,⁸ Elena E. Giorgi,⁹ James Theiler,⁹ Kathleen B.J. Pommert,¹ Tyler B. Krause,⁴ Hannah L. Turner,² Charles D. Murin,² Jesper Pallesen,² Edgar Davidson,¹⁰ Rafi Ahmed,¹¹ M. Javad Aman,¹² Alexander Bukreyev,¹³ Dennis R. Burton,¹ James E. Crowe, Jr.,¹⁴ Carl W. Davis,¹¹ George Georgiou,¹⁵ Florian Krammer,¹⁶ Christos A. Kyrtasous,¹⁷ Jonathan R. Lai,⁵ Cory Nykiforuk,¹⁸ Michael H. Pauly,¹⁹ Pramila Rijal,²⁰ Ayato Takada,²¹ Alain R. Townsend,²⁰ Viktor Volchkov,²² Laura M. Walker,²³ Cheng-I. Wang,²⁴ Larry Zeitlin,¹⁹

(Author list continued on next page)

¹Department of Immunology and Microbiology

²Integrative Structural and Computational Biology

The Scripps Research Institute, La Jolla, CA 92037, USA

³Ragon Institute, Cambridge, MA 02139, USA

⁴Department of Microbiology and Immunology

⁵Biochemistry

Albert Einstein College of Medicine, Bronx, NY 10461, USA

⁶Division of Pathobiological Sciences, University of Wisconsin, Madison, WI 53706, USA

⁷Division of Virology, United States Army Research Institute for Infectious Diseases, Ft. Detrick, MD 21702, USA

⁸National Microbiology Laboratory, Public Health Agency of Canada, Winnipeg R3E 3R2, Canada

⁹Los Alamos National Laboratory, Los Alamos, NM 87545, USA

¹⁰Integral Molecular, Philadelphia, PA 19104, USA

¹¹Emory Vaccine Center, Emory University School of Medicine, Atlanta, GA 30322, USA

¹²Integrated BioTherapeutics, Rockville, MD 20850, USA

¹³Galveston National Laboratory, University of Texas Medical Branch, Galveston, TX 77555, USA

¹⁴Vanderbilt Vaccine Center, Vanderbilt University Medical Center, Nashville, TN 37232, USA

¹⁵Department of Chemical Engineering, University of Texas at Austin, Austin, TX 78712, USA

¹⁶Department of Microbiology, Icahn School of Medicine at Mount Sinai, New York, NY 10029, USA

¹⁷Regeneron Pharmaceuticals, Inc., Tarrytown, NY 10591, USA

¹⁸Emergent BioSolutions, Winnipeg, Manitoba, R3T 5Y3, Canada

¹⁹Mapp Biopharmaceutical, San Diego, CA 92121, USA

(Affiliations continued on next page)

SUMMARY

Antibodies are promising post-exposure therapies against emerging viruses, but which antibody features and *in vitro* assays best forecast protection are unclear. Our international consortium systematically evaluated antibodies against Ebola virus (EBOV) using multidisciplinary assays. For each antibody, we evaluated epitopes recognized on the viral surface glycoprotein (GP) and secreted glycoprotein (sGP), readouts of multiple neutralization assays, fraction of virions left un-neutralized, glycan structures, phagocytic and natural killer cell functions elicited, and *in vivo* protection in a mouse challenge model. Neutralization and induction of multiple immune effector functions (IEFs) correlated most strongly with protection. Neutralization predominantly occurred via epitopes maintained on endoso-

mally cleaved GP, whereas maximal IEF mapped to epitopes farthest from the viral membrane. Unexpectedly, sGP cross-reactivity did not significantly influence *in vivo* protection. This comprehensive dataset provides a rubric to evaluate novel antibodies and vaccine responses and a roadmap for therapeutic development for EBOV and related viruses.

INTRODUCTION

Unexpected viral disease outbreaks, such as Ebola virus disease, underscore the need for effective vaccines and therapies. Antibodies are a primary correlate of protection of most approved vaccines and can serve as pre- or post-exposure treatment strategies. Although antibody-mediated neutralization of virus in cell culture is commonly used to predict *in vivo* antiviral protection, non-neutralizing, but cell-targeting antibodies also confer *in vivo* protection (Henry Dunand et al., 2016; Lewis



Benjamin J. Doranz,¹⁰ Andrew B. Ward,² Bette Korber,⁹ Gary P. Kobinger,^{25,*} Kristian G. Andersen,^{1,*} Yoshihiro Kawaoka,^{6,*} Galit Alter,^{3,*} Kartik Chandran,^{4,*} and John M. Dye^{7,*} the Viral Hemorrhagic Fever Immunotherapeutic Consortium²⁶

²⁰Human Immunology Unit, University of Oxford, Oxford OX3 9DS, UK

²¹Research Center for Zoonosis Control, Hokkaido University, Sapporo 001-0020, Japan

²²INSERM CNRS, Université Lyon, Lyon, France

²³Adimab, LLC, Lebanon, NH 03766, USA

²⁴Singapore Immunology Network, Agency for Science, Technology and Research (A*STAR), Biopolis 138648, Singapore

²⁵Département de Microbiologie-Infectiologie et d'Immunologie, Médecine, Université Laval Québec, G1V 046 Canada

²⁶<https://vhfimmunotherapy.org/>

²⁷These authors contributed equally

²⁸Lead contact

*Correspondence: erica@scripps.edu (E.O.S.), gary.kobinger@crchudequebec.ulaval.ca (G.P.K.), andersen@scripps.edu (K.G.A.), kawaokay@svm.vetmed.wisc.edu (Y.K.), galter@mgm.harvard.edu (G.A.), kartik.chandran@einstein.yu.edu (K.C.), john.m.dye1.civ@mail.mil (J.M.D.)

<https://doi.org/10.1016/j.cell.2018.07.033>

et al., 2017). Understanding which antibody features correlate with protection *in vivo* could accelerate discovery and provision of protective therapeutics.

The surface glycoprotein (GP) of Ebola virus (EBOV) is the key component of vaccines and target of neutralizing antibodies. In producer cells, furin cleaves GP to yield GP1 and GP2 (Sanchez *et al.*, 1998), which form a trimer of GP1-GP2 heterodimers on the viral surface (Lee *et al.*, 2008). GP1 bears the receptor-binding site, glycan cap, and mucin-like domain. GP2 bears an N-terminal peptide, internal fusion loop, stalk, and transmembrane domain (Lee *et al.*, 2008). After internalization of virions into target cells, host cathepsins (Chandran *et al.*, 2005; Schornberg *et al.*, 2006) remove the glycan cap and mucin-like domain to expose the receptor-binding site at the GP1 apex (Miller *et al.*, 2012) and form GP_{CL}, the endosomal cleaved form of GP that allows receptor binding (Chandran *et al.*, 2005; Dube *et al.*, 2009). After receptor binding, GP2 rearranges to form a six-helix bundle that promotes membrane fusion.

During Ebola virus infection the primary product of the GP gene is secreted GP (sGP), a soluble dimer that lacks GP2 and the mucin-like domain but shares 295 amino acids of GP1 (Sanchez *et al.*, 1996).

Previous studies described monoclonal antibodies (mAbs) that target various sites on GP and sGP, including the “base,” comprising both GP1 and GP2, the GP2 fusion loop and stalk (HR2), and the GP1 receptor-binding head, glycan cap and mucin-like domain (Audet *et al.*, 2014; Bornholdt *et al.*, 2016; Corti *et al.*, 2016; Dias *et al.*, 2011; Lee *et al.*, 2008; Marzi *et al.*, 2012; Shedlock *et al.*, 2010; Wilson *et al.*, 2000). Antibodies recognizing the GP1 head and glycan cap also bind sGP.

The mechanistic basis for differences in neutralization and *in vivo* protection among mAbs is unclear. For example, the GP-specific antibodies KZ52, 2G4, and 4G7 all recognize overlapping epitopes at the GP base (Lee *et al.*, 2008; Murin *et al.*, 2014), neutralize *in vitro*, and are escaped by the Q508R point mutation (Audet *et al.*, 2014; Qiu *et al.*, 2012). KZ52 monotherapy failed to protect non-human primates (NHPs) (Oswald *et al.*, 2007), but a cocktail of 2G4 and 4G7 and the weakly neutralizing, partially protective, GP/sGP cross-reactive mAb 13C6 protected NHPs (Qiu *et al.*, 2014). The cocktail MB-003 has only non- and weakly neutralizing antibodies that target glycan cap or mucin

epitopes, but it provided protection to NHPs (Olinger *et al.*, 2012). Further, mAb 114, recognizing both GP and sGP, protected NHPs as a monotherapy (Corti *et al.*, 2016).

What features beyond epitope recognition and neutralization associate with protection remain unclear, as is whether single mAbs or cocktails provide optimal therapeutic benefit and the extent to which cross-reactive protection is possible. Further, neutralization capacity differs among assays. Better understanding of features that confer protection, what assays best predict survival, and what combinations of antibody features provide optimal protection could streamline selection of effective treatments.

In 2013 the Viral Hemorrhagic Fever Immunotherapeutic Consortium (VIC) began gathering antibodies to EBOV and other viruses and analyzing them under identical assay conditions to understand, from a more statistically well-powered pool, which antibodies are best and why (Saphire *et al.*, 2017). A parallel goal was to evaluate the assays themselves to determine which *in vitro* tests and measurable antibody features best predict *in vivo* efficacy.

The 171 mAbs analyzed included murine mAbs raised by immunization, chimeric mAbs, and human survivor mAbs from the 1995 EBOV, 2007 Bundibugyo (BDBV), and 2013-2016 EBOV outbreaks. Also included were ZMapp (Qiu *et al.*, 2014), KZ52 (Maruyama *et al.*, 1999), and other published and unpublished mAbs (Bornholdt *et al.*, 2016; Flyak *et al.*, 2016; Fusco *et al.*, 2015; Holtsberg *et al.*, 2015; Keck *et al.*, 2015; Koellhoffer *et al.*, 2012; Pascal *et al.*, 2018; Qiu *et al.*, 2012; Takada *et al.*, 2003; Wilson *et al.*, 2000). The study results describe relationships between epitopes recognized on EBOV GP and antibody functions and inform strategies for recognition and development of effective antibody-based therapeutics to treat infection.

RESULTS

Antibody Standardization and Characterization

We analyzed 171 mAbs donated by 16 investigators for isotype, species, and EBOV GP reactivity. A total of 168 mAbs were analyzed after elimination of 3 mAbs that had low sample quality or GP purification tag reactivity. The sample pool included 102 human mAbs (94 IgG1, 1 IgG3, 5 chimerized to IgG1, 2

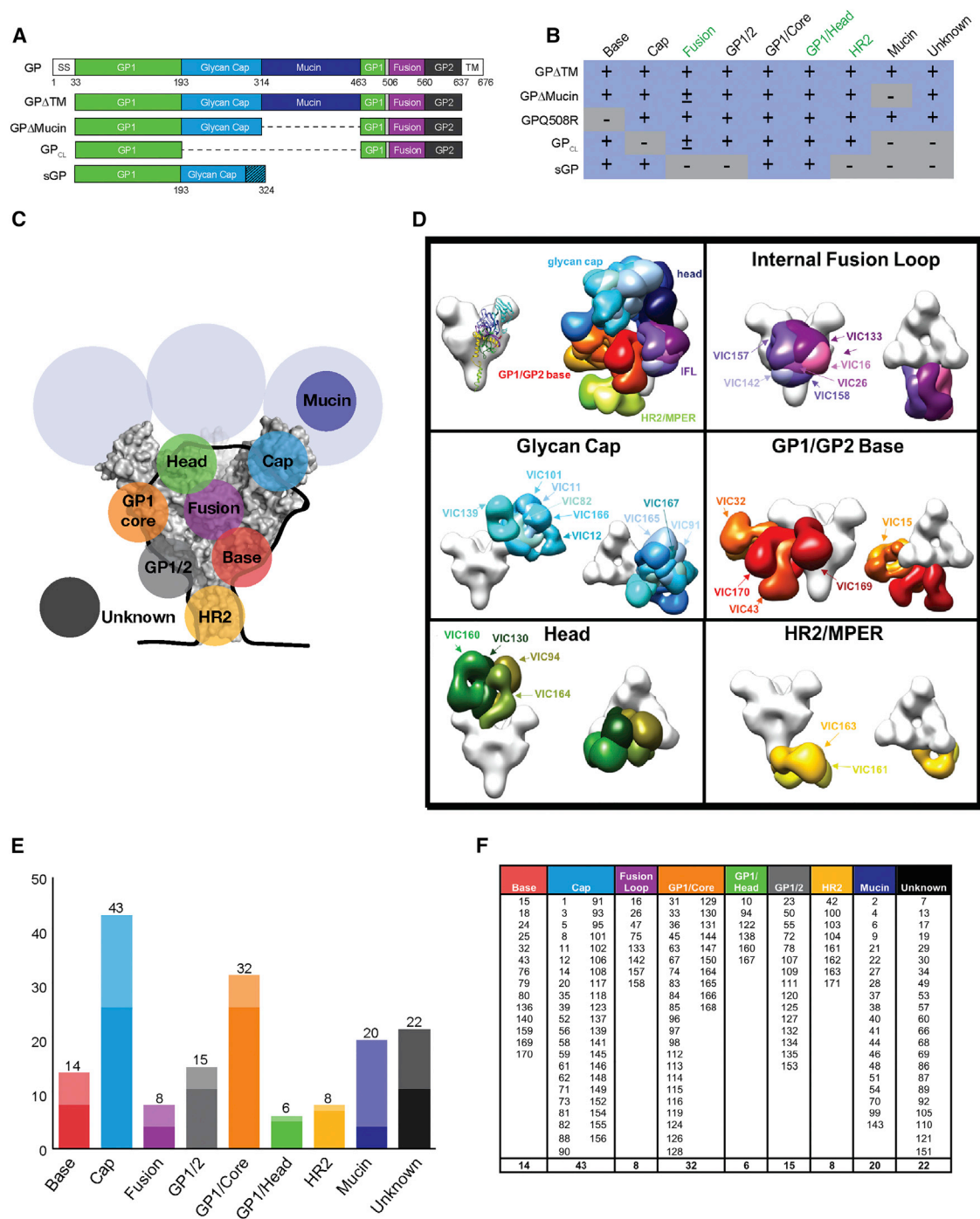


Figure 1. VIC Antibody Epitope Distribution

(A) Recombinant full-length and fragments of Ebola virus GP (Mayinga) used to assess antibody binding by ELISA.

(B) ELISA binding in which +, -, and ± indicate binding, no binding, and either weak or inconsistent binding, respectively. GP Q508R abolishes GP base binding. Some epitope classes (green labels) were later assigned by alanine scanning mutagenesis and electron microscopy analysis.

(C) Space-filling diagram of EBOV GPΔMuc (PDB 3CSY) with epitope classes colored according to the histogram. The mucin domain structures were not resolved and are shown as blue circles. GP1/Core encompasses several regions of the GP structure and is not shown.

(D) Single-particle negative-stain reconstructions of selected VIC panel antibodies fit to EBOV GPΔMuc (PDB 3CSY). GP1 (blue and cyan) and GP2 (yellow and green) domains are represented by ribbon diagrams (top left panel). Core GPs and Fabs are shown as surfaces in white and various colors, respectively. Fab densities were fit to a model Fab and a side view is shown.

(legend continued on next page)

undetermined) and 66 murine mAbs (20 IgG1, 37 IgG2a, 8 IgG2b, 1 IgG3) (Figure S1).

Epitope Characterization

We first assessed ELISA reactivity of the mAbs to different forms of recombinant EBOV GP and sGP (Mayinga), including: (1) GP ectodomain (GP Δ TM, referred to below as GP), (2) mucin-deleted ectodomain (GP Δ muc), (3) thermolysin-cleaved GP (GP Δ CL, mimicking cathepsin-primed GP), (4) GP bearing a Q508R escape mutation (Audet et al., 2014), and (5) sGP (Figure 1A).

A total of 79 mAbs had sGP cross-reactivity, of which 39 bind the glycan cap and 40 the GP1 core. The other 89 had epitopes distributed across the mucin-like domain, the “base” and GP Δ CL core regions. ELISA reactivity was insufficient to map epitopes for 30 mAbs, but 8 (1 base, 2 glycan cap, 2 HR2, and 3 fusion loop binding mAbs) were resolved using single particle electron microscopy and alanine scanning (Figures 1, S1, and Table S1).

After refinement, nine epitope classes were defined: mucin-like domain, glycan cap, GP1 head, GP1/GP2 trimer base, GP1 Core, GP1/2, fusion loop, HR2 stalk, and unknown binding sites (Figures 1E and 1F).

Three Independent Assays for Evaluation of mAb Neutralization

Disparities in previous antibody-mediated neutralization results could be due to differing experimental conditions and model systems (Davidson et al., 2015; Li et al., 2016; Wilkinson et al., 2017; Wilson et al., 2000). Thus, we characterized the neutralization of each mAb in three assays: (1) replication-competent vesicular stomatitis virus bearing EBOV GP (rVSV); (2) biologically contained EBOV (Δ VP30) (Halfmann et al., 2008); and (3) authentic EBOV (Figure 2) performed under BSL-2+, BSL-3, and BSL-4 containment, respectively, as previously described, to ensure consistency with previous studies. Of the 168 mAbs, 96 registered as consistent non-neutralizers (no neutralization e.g., VIC 1, Figure 2A), 45 as consistent neutralizers (neutralize in every assay to some degree, e.g., VIC 8), and 27 as inconsistent neutralizers (neutralize in only some assays, e.g., VIC 12). Of the 27 inconsistent neutralizers, 12 varied by a smaller degree (moderate to non-neutralizing, e.g., VIC 104 in HR2), while 15 varied by a larger degree (potent to non-neutralizing, e.g., VIC 5 in glycan cap). Inconsistent neutralizers varied among the experimental systems in both degree of neutralization and which model system was neutralized. Thus, mAb selection using a single neutralization assay is a functional but imperfect funnel.

Several trends emerged. The authentic EBOV assay was more forgiving: 15 mAbs neutralized only EBOV. Δ VP30 was more stringent: 11 mAbs neutralized EBOV and rVSV, but not Δ VP30 (Figure 2A). Interestingly, these 11 left a larger (2%–40%; median 20%) un-neutralized viral fraction in rVSV (Figure 2A), which could indicate low binding affinity or an epitope heterogeneous in conformation or glycosylation state. This heterogeneity in

antigenic presentation may underlie previously observed differences among neutralization assay results for the same mAb and could be an important component in selecting therapeutic mAbs.

Neutralization by glycan cap mAbs in particular differed between authentic EBOV and the two model systems. Among mAbs that only neutralize authentic EBOV, 9/15 recognize the glycan cap (Figure 2A). Further, for authentic EBOV, the mean neutralization value for glycan cap mAbs was significantly higher than that of mucin, GP1/2, and unknown epitopes (Figures 2B–2E).

An important difference among the three neutralization assays was the presence of sGP. The rVSV system is engineered to prevent sGP expression, but Δ VP30 and authentic EBOV assays express wild-type sGP levels (Volchkov et al., 1995). As such, we expected sGP-reactive mAbs (e.g., glycan cap) to exhibit stronger neutralization in the rVSV assay. Paradoxically, only 2/43 glycan cap antibodies (VIC 5 and 81) had stronger neutralization in rVSV, whereas 11/43 had weaker rVSV neutralization than in sGP-containing assays.

Relationship of Epitope to Neutralization

For mAbs against GP1, neutralization potency varied by the GP1 region recognized. Only 1/20 mucin mAbs neutralized in any assay. In contrast, 5/6 mAbs against the GP1 head, near the receptor-binding site, neutralized. Glycan cap mAbs were more variable: 21/43 were non-neutralizing and 9/43 had strong or moderate activity in all assays (Figure 2). mAbs against GP2-containing epitopes typically had high neutralizing activity: 26/30 showed strong neutralizing activity in at least two assays. Overall, mAbs recognizing the GP1 head, fusion loop, base, and HR2 present in GP Δ CL were more likely to neutralize than mAbs targeting GP regions removed by enzymatic cleavage (Figure 2).

mAbs having undefined epitopes did not neutralize well: 19/22 of unknown epitope and 12/15 mAbs in the GP1/2 class (bind GP Δ CL, but could not be assigned as base, fusion, or stalk), did not neutralize at all.

In natural infection, abundant sGP could limit effective neutralization of circulating virus by sGP-cross-reactive antibodies (Illyin et al., 2016; Mohan et al., 2012) (Figure 2). However, as mentioned above, we typically saw equivalent or weaker relative neutralization in rVSV relative to the sGP-containing Δ VP30 and EBOV assays. Further, the sGP-cross reactive glycan cap group constitutes the majority of the discordant antibodies that did not neutralize rVSV at all, but did neutralize in the sGP-containing authentic EBOV assay. Thus, the presence of sGP does not itself appear to be detrimental to neutralization of sGP-reactive mAbs.

Relationship of Epitope to Protection

We next assessed whether each of the 168 mAbs could confer protection to BALB/c mice inoculated with mouse-adapted Ebola virus (ma-EBOV; Mayinga variant) (Bray et al., 1998). Groups of 10 mice each received one 100 μ g mAb dose two

(E) VIC mAb epitope classes. The total number of mAbs in each epitope class is shown; lighter shading represents murine mAbs.

(F) VIC panel mAb epitope classes.

The color coding scheme is used in all figures.

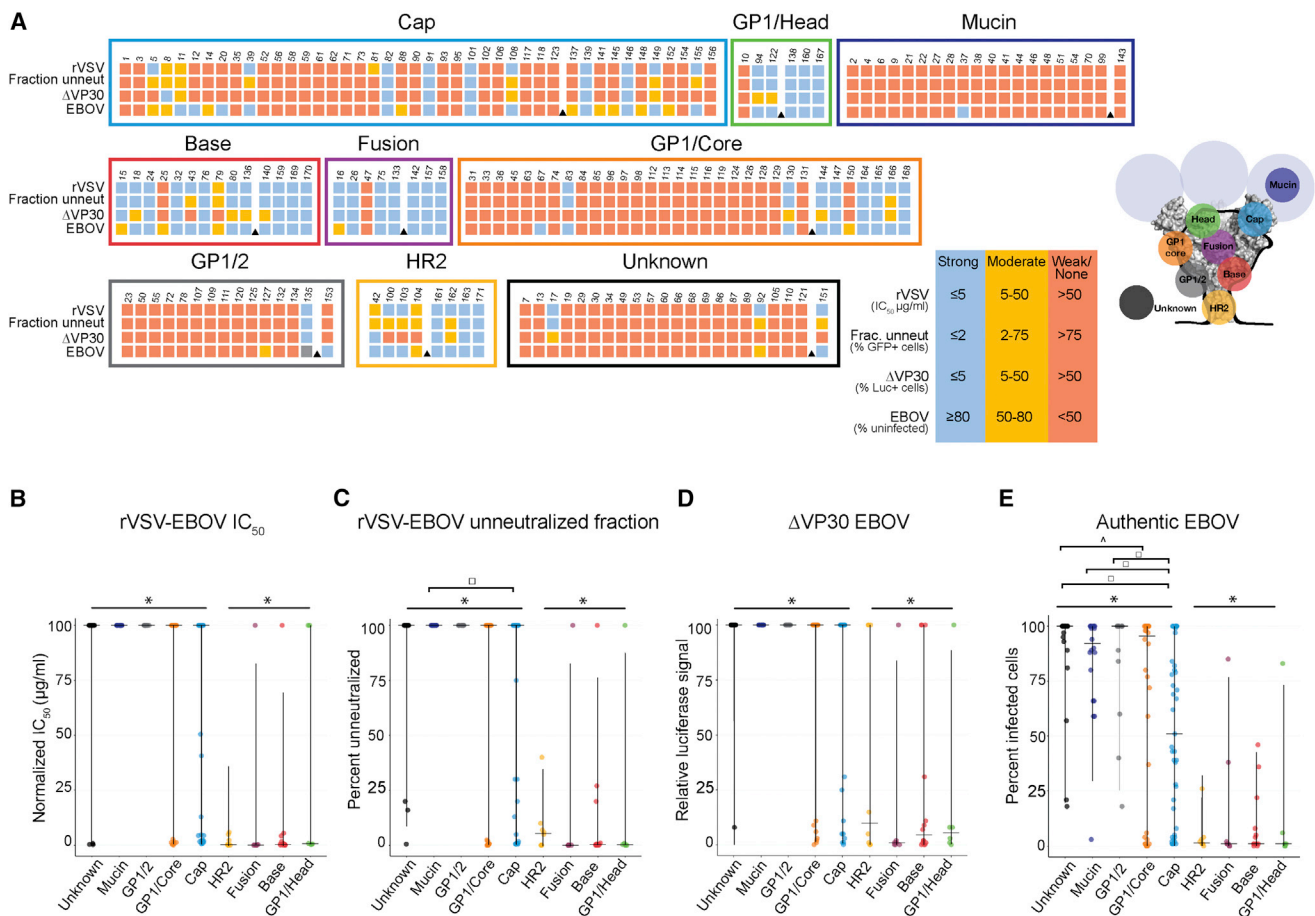


Figure 2. Comparison of Neutralization Assay Results

(A) Results are color-coded according to the ranges listed. mAbs are grouped by epitope class and arranged by position on the GP structure. The EBOV GP structure is shown and the black line outlines regions remaining in GP_{CL}. mAbs to the right of the black triangles were donated after the epidemic. (B–E) Correlation between epitope class and neutralization assay results by parametric ANOVA shown as modified boxplots. Vertical lines represent distribution between first and third quartiles; horizontal lines indicate the mean value. Asterisks, squares, and carats indicate significantly different mean values with $p < 0.04$.

days after challenge with ma-EBOV. Protection levels of 60%–100%, 40%–50%, and <40% were seen for 49, 16, and 103 mAbs, respectively (Figure 3, S3, Table S2).

Among mAbs with assigned epitopes, 16/69 GP1-reactive and 21/30 GP2-reactive mAbs protected to $\geq 60\%$. Among GP1-containing epitopes, 5/6 GP1/Head, 9/32 GP1/core, 10/43 glycan cap, and 1/20 mucin-like domain mAbs conferred $\geq 60\%$ protection (Figures 3A and S3). Of GP2-containing epitopes, 6/8 fusion loop, 10/14 base, and 6/8 HR2 conferred $\geq 60\%$ protection. Of mAbs lacking specific epitopes, 9/32 GP1/core, 1/15 GP1/2, and 2/22 antibodies with unknown epitopes were protective (Figures 3A and S3). Although mAbs against the GP1/Head, base, fusion loop, and HR2 had significantly higher mean protection values (Figure 3B), every epitope class contained at least one mAb that conferred high ($\geq 80\%$) protection.

Relationship of Neutralization to Protection

Although non-neutralizing antibodies can offer *in vivo* protection from Ebola and other viruses (Haynes et al., 2012; Henry Dunand

et al., 2016; Horwitz et al., 2017; Lewis et al., 2015; Olinger et al., 2012; Wilson et al., 2000), neutralization is often the primary selector of mAbs for *in vivo* evaluation. Here we aimed to cast a broad net across this mAb panel to measure correlation between *in vitro* neutralization and protection in the mouse model.

In each assay, neutralization potency showed a high and statistically significant correlation with protection. This relationship was the strongest for fraction of rVSV left unneutralized (Spearman's $\rho = -0.068$) and rVSV IC₅₀ ($\rho = 0.67$), followed by the percentage of infected cells in the authentic EBOV assay ($\rho = 0.65$) and fraction ΔVP30 neutralized ($\rho = 0.61$).

By unsupervised K-means clustering analysis, we clustered the mAbs by neutralization results, then independently co-plotted protection values (Figure 4). The five clusters contained mAbs that: (1) were non-neutralizing, (2) failed to neutralize ΔVP30, (3) only neutralize authentic EBOV, (4) neutralize model systems better than EBOV, and (5) neutralize in all assays. Although there were general trends (88% of consistently non-neutralizing antibodies do not protect, while 89% of the consistently neutralizing antibodies do), each cluster had a range of

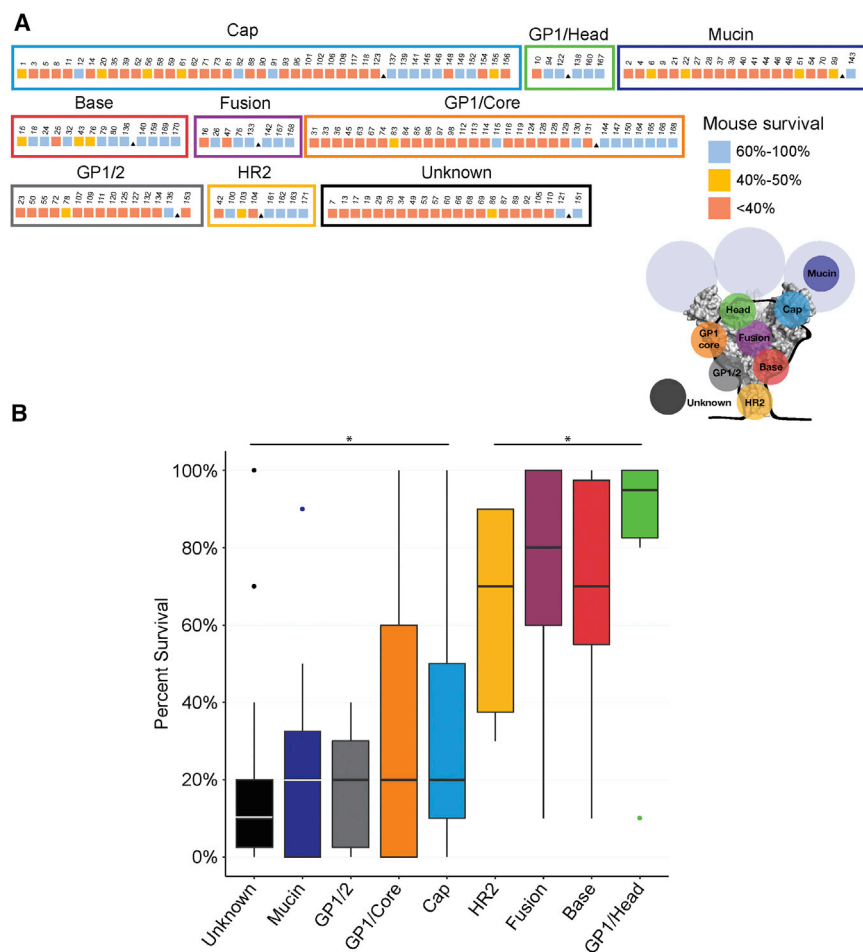


Figure 3. Relationship between *in vivo* Protection and Epitope Class for VIC mAb Panel

(A) Groups of 10 mice were infected with ma-EBOV and treated with 100 μ g/ml of the indicated mAb on day 2 post-infection. The final percentage of surviving animals is indicated.

(B) Parametric analysis of correlation between epitope class and protection. Black and white bars indicate mean values. The mean values for HR2, fusion, base, and GP1/Head differed significantly from those for unknown, mucin, GP1/2, GP1/Core, and cap ($p \leq 0.0026$).

protective activity. For cluster 1, 9% of non-neutralizing mAbs were moderately protective and another 3.3% were more highly protective (VIC 115, VIC 121 and VIC 143). In cluster 5, VIC 42, VIC 76, VIC 101, and VIC 108 neutralized robustly but protected $\leq 50\%$. Selecting by neutralization alone would thus identify most, but not all, protective antibodies. Further, comparison of cluster 5 to 2–4 suggests that protection is best identified by the ability to neutralize in several distinct systems.

Binding to Other Filovirus GPs and Mouse Adapted-Ebola Virus

Neutralization assays were performed using virions bearing wild-type EBOV GP, whereas protection studies used ma-EBOV bearing three GP point mutations (S65P, S246P, and I544T) (Ebihara et al., 2006). mAb reactivity did not significantly differ between wild-type and ma-EBOV GP by ELISA, including those mAbs that neutralized wild-type GP in culture but did not protect *in vivo* (Figure S4). Thus, use of ma-EBOV does not explain the failure of these neutralizing mAbs to confer protection.

ELISA assessment of VIC panel mAb binding to the GP ectodomain of West African (i.e., Makona) and Central African (i.e.,

Mayinga) EBOV, Bundibugyo virus (BDBV), Reston virus (RESTV), Sudan virus (SUDV) and Marburg virus Ravn (RAVV) showed that most mAbs in the panel (91%) bound Mayinga and Makona GP equally well (Figure 5). Nine, distributed across six epitope groups, had reduced binding to Makona GP. Makona-related substitutions thus affected a minority of mAbs, but at a variety of epitopes.

A total of 75/168 mAbs recognized at least one other filovirus GP, and 27 had pan-ebolavirus reactivity. Fusion loop mAbs were most frequently fully cross-reactive, followed by those targeting GP1/Head, GP1/Core and HR2. No mucin mAbs were cross-reactive. Of the cross-reactive antibodies, 24 neutralized in at least two of the three EBOV neutralization assays performed and 25 conferred $\geq 60\%$ protection.

VIC 78, 98, 109, and 111 cross-reacted with marburgvirus Ravn GP on ELISA (Figure 5), but no EBOV/RAVV cross-reactive mAb had strong protection or neutralization activity.

Immune Effector Function of VIC Panel mAbs Association of Fc-Mediated Effector Functionality with mAb-Mediated Protection

The finding that several mAbs afforded *in vivo* protection but showed little *in vitro* neutralization activity suggests that protection involves other factors. Thus, we measured the ability of mAbs to engage the innate immune system via induction of seven different immune effector functions (IEFs).

Phagocytosis removes pathogen-infected cells and can be mediated by monocytes, macrophages, dendritic cells, and neutrophils. To account for differences in antibody subclasses and FcR engagement (Bruhns, 2012), we obtained four different phagocytosis readouts: antibody-dependent cellular phagocytosis (ADCP) by human and mouse monocytes and antibody-dependent neutrophil phagocytosis (ADNP) by human and mouse neutrophils, with phagocytic scores for each mAb calculated as described in the Methods.

Most VIC mAbs ($< 75\%$) induced ADCP, yet only 30% induced ADNP (Figure 6). In all four assays, Tier 1, the outermost region of

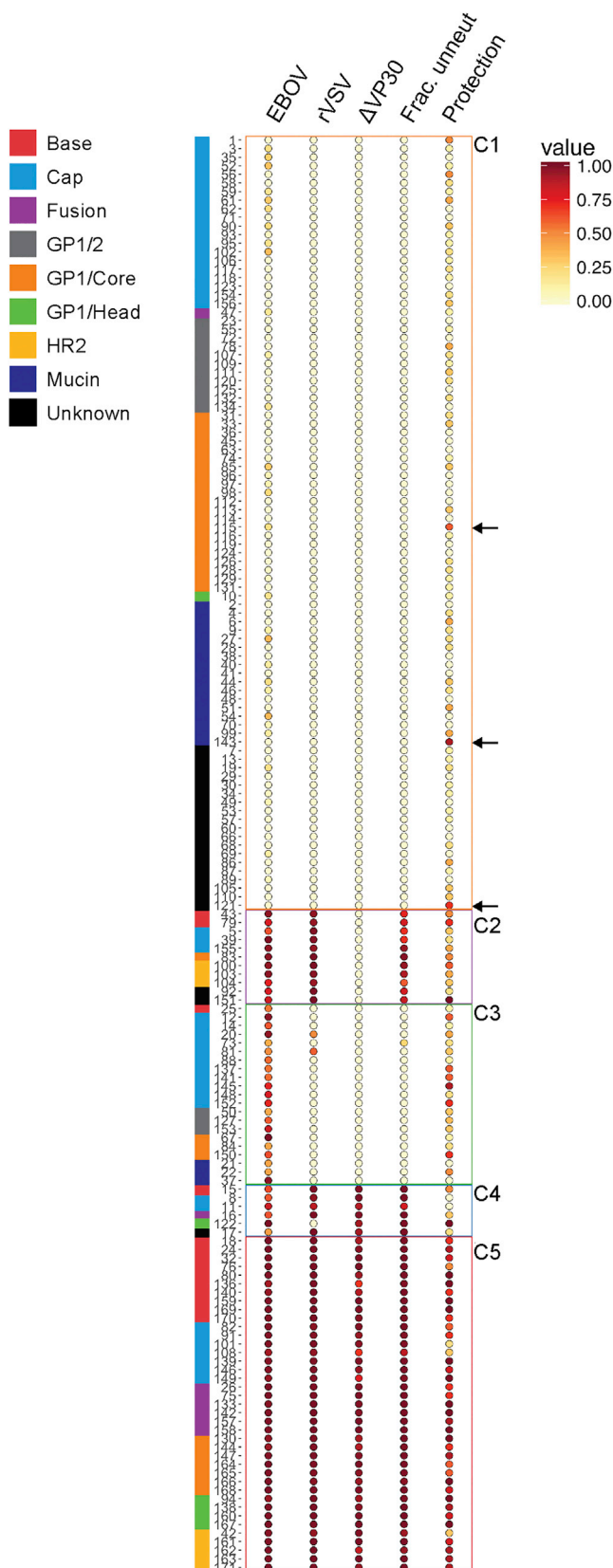


Figure 4. K-Means Clustering of VIC mAb Neutralization Readouts

Clusters C1-C5 are based on neutralization activity (normalized with 1.0 as the maximum value). *In vivo* protection results are shown for reference. VIC 115, 121, and 143 (arrows) protect but do not neutralize.

the GP molecule with respect to the virus membrane that encompasses the mucin, glycan cap, and GP1/Head groups, had the highest phagocytic activity relative to Tiers 2 (base, fusion, and GP1/Core) and 3 (GP1/2 and HR2). Furthermore, the glycan cap epitope class induced significantly more phagocytic activity compared to other epitope classes (Figure 6, S5A–S5D).

Natural killer (NK) cells play a key role in antiviral immunity by directly killing infected cells or secreting chemokines and cytokines to activate immune signaling pathways (Waggoner et al., 2016). NK-mediated ADCC requires release of cytotoxic granules (i.e., degranulation) that kill antibody-opsonized cells. Surface CD107a is a marker of NK degranulation (Alter et al., 2004). Secreted cytokines and chemokines such as IFN γ and MIP-1 β also confer antiviral effects of NK (Oliva et al., 1998). Among the 168 mAbs, 33 induced moderate to strong levels of all three NK markers (Figure 6). Ten, across seven epitope groups, strongly activated all three NK functions and 6/10 protected to $\geq 60\%$. Of these, four were also strong neutralizers, whereas VIC 100 (HR2) did not neutralize VP Δ 30 and VIC 143 (mucin) had no neutralization activity. A second group of 10 mAbs elicited high levels of IFN γ and MIP-1 β , but not CD107a. Of these, five protected to $\geq 60\%$ and three had strong neutralization activity, whereas VIC 137 and 141 neutralized only authentic EBOV.

Base and GP1/Head mAbs had higher average NK scores than other epitope classes (Figure 6).

Fc Polyfunctionality of VIC Panel mAbs

Polyfunctionality (PF) describes the ability of an antibody to recruit multiple IEFs and is associated with increased vaccination efficacy (Ackerman et al., 2016; Chung et al., 2014). Here, PF was scored from 0–7, with one point for each phagocytic or NK function having activity above a defined threshold relative to a control mAb (Figure 6). Among the panel, 29 (mostly human) mAbs induced 6 or 7 effector functions, while 33 mAbs (18 human IgG1, 15 murine [12 IgG1, 2 IgG2a, 1 IgG2b]) evoked 0 or 1 IEF.

PF was significantly positively correlated with protection ($p = 8.03 \times 10^{-6}$). Among the 48 mAbs that conferred $\geq 60\%$ protection, the average PF score was 4.0, compared to 2.7 for mAbs with lower protection activity. Among non-protective mAbs, 11 induced no IEFs, whereas all protective group mAbs induced at least one IEF (Figure 6).

The mucin epitope group had the highest average PF score of 3.95 and all elicited at least 2 IEFs, with 80% eliciting ≥ 4 . GP1/Head and glycan cap mAbs had average PF scores of 3.7 and 3.5, respectively (Figure S5E).

Glycosylation and mAb function

Capillary electrophoresis analysis showed that VIC mAbs had notable heterogeneity in the relative abundance of specific glycans (Table S3). G0F, G2S1FB, and total G0 glycosylation levels were positively associated with protection, whereas

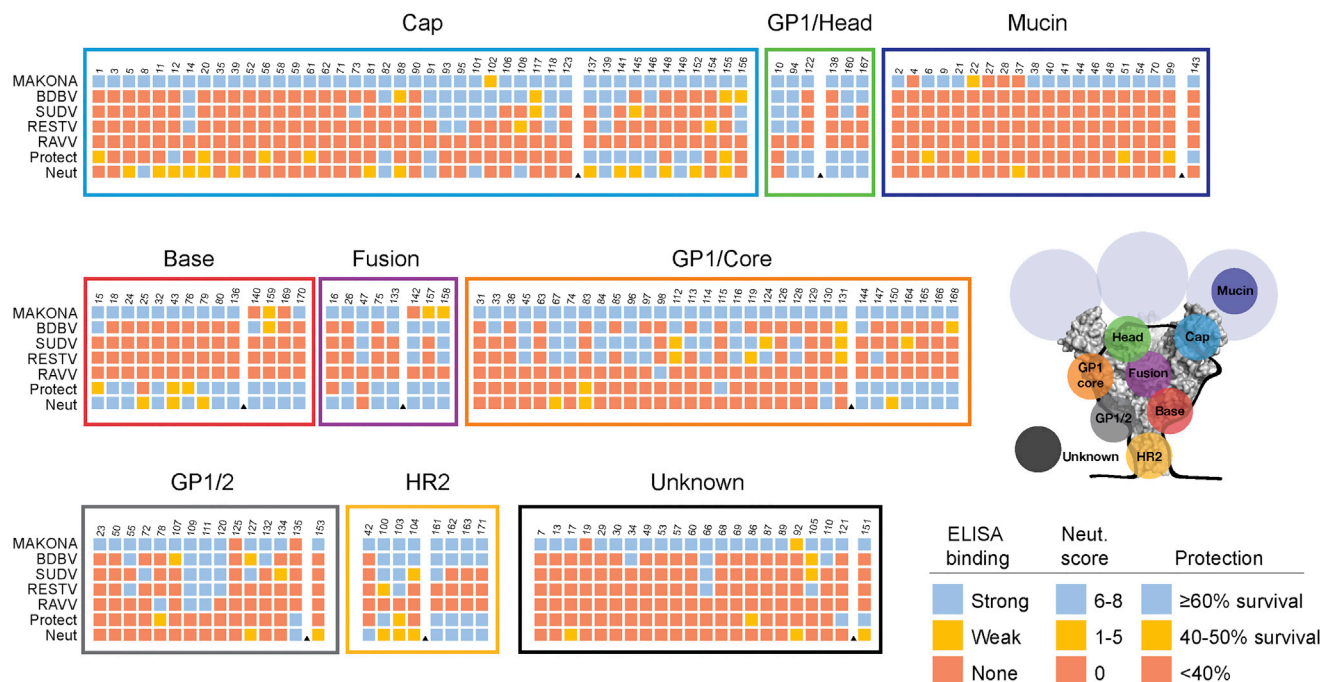


Figure 5. ELISA Cross-Reactivity of VIC mAbs with GP of Other *Ebolavirus* Species

ELISA cross-reactivity of VIC mAbs with GP of other *Ebolavirus* species (Bundibugyo virus, BDBV; Sudan virus, SUDV; Reston virus, RESTV) and the marburgvirus Ravn virus (RAVV). Strong, moderate, and weak/no neutralization were scored as 2, 1, and 0, respectively, in the four assays.

G2S1 and G1S1F had a negative association (Figures 7A and 7B). Mucin-specific mAbs had higher levels of G1F' and total G1 glycans, consistent with the reduced protective efficacy seen for this class (Figures S6C and S6E). GP1/Head mAbs were more likely to have G0F and had the lowest amounts of total G1 (Figures S6A and S6E), consistent with the elevated protective efficacy of this epitope group (Figure 3). Fc functions and glycans are analyzed in greater detail in a companion publication (Gunn et al., 2018).

Regression Analysis of VIC Antibody Function Correlation Network

We used pairwise Spearman's ρ correlation coefficients to identify pairwise relationship(s) between all measured mAb features. The resulting correlation network (<http://apps.vhfimmunotheapy.org/cornetwork>; <http://apps.vhfimmunotheapy.org/vic-data-explorer/>) allows visualization of relationships between protection and single mAb features, as well as identification of the multiple mAb features that together could contribute to a given functional response or protection. As expected, protection had a strong positive correlation with all four neutralization readouts ($\rho = 0.61$ – 0.68) and a moderate positive correlation with polyfunctionality ($\rho = 0.35$).

Neutralization activity was positively associated with base, fusion, and HR2 mAbs (Tiers 2 and 3) and negatively associated with mAbs targeting the mucin domain. In contrast, phagocytosis, and thus total PF, were positively associated with Tier 1 epitopes ($\rho = 0.31$). NK functions, however, linked neither to tier nor epitope. Both neutralization and PF were improved by

stronger binding to GP: lower EC₅₀ values correlated with greater neutralization and higher PF.

Neutralization activity had a weak positive and negative, respectively, correlation with Total G0 ($\rho = 0.21$ – 0.28) and G2F ($\rho = -0.2$ – 0.26), whereas Total G1 had a weak negative correlation only with rVSV ($\rho = -0.26$) and Δ VP30 ($\rho = -0.25$). PF was positively associated with the glycan modifications G1 ($\rho = 0.24$), G2S1FB ($\rho = 0.26$), and G2S1B ($\rho = 0.33$), and negatively associated with G2S1F ($\rho = -0.29$), total fucose ($\rho = -0.26$), and total sialic acid ($\rho = -0.23$). Of the IEFs, NK activity was most negatively associated with G2S1F, but boosted by afucosylated G2S1B, consistent with afucosylation as a driver of Fc γ R1IIa-mediated NK cell activation (Shields et al., 2002).

Features Predictive of Antibody Protection

We built and evaluated multivariate models of protection using four machine learning algorithms. Logistic regression with elastic net regularization (LR) (Zou and Hastie, 2005) performed best (AUC = 0.959, Figure S7A) and generated a multivariate model of protection employing 17 mAb features (Figure 7B). Random forest (RF) regression with 10-fold cross-validation showed that this approach predicted protection conferred by the VIC panel mAbs with reasonable accuracy (mean absolute error = 16.1%; Figure S7B). Ranking the importance of features for RF predictions supports a dominant role for the three neutralization assays followed by mAb PF (Table S4). Other effector, glycan, and binding variables were incorporated in the RF regression predictions, but their contribution was not substantial (feature importance < 0.02).

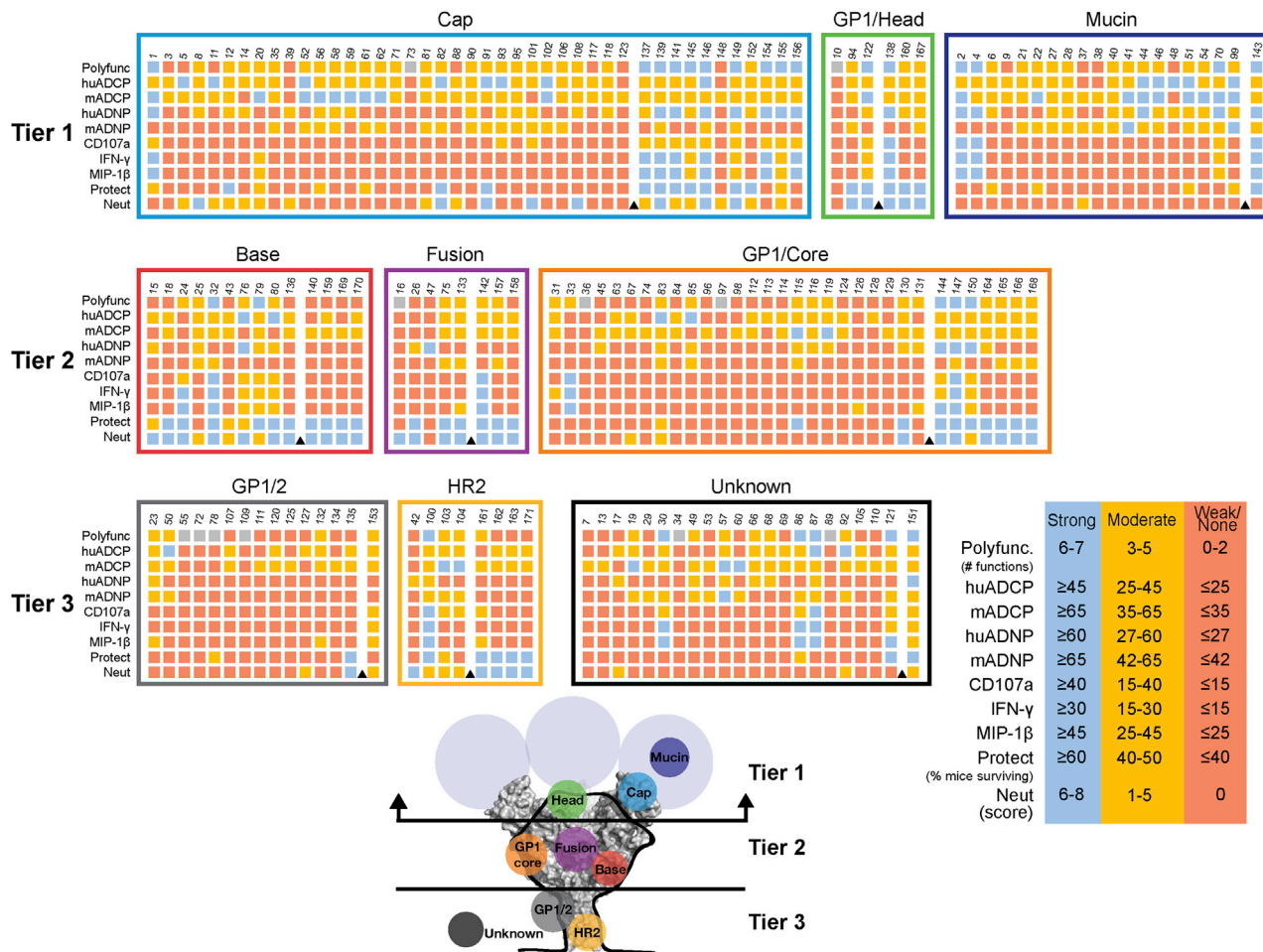


Figure 6. Immune Effector Functions and VIC mAb Polyfunctionality

Induction of phagocytosis activity in mouse and human monocytes and neutrophils (huADCP, huADNP and mADCP, mADNP) and NK cell activation (IFN γ and MIP-1 β secretion; CD107a surface exposure) was measured for each mAb. Polyfunctionality scores ranged from 0–7, with one point given for strong or moderate activity on each of seven readouts. Tier 1 epitopes lie the farthest from the membrane.

Although unneutralized fraction of rVSV had the strongest correlation with *in vivo* survival in RF analyses, it is, by itself, not always an accurate predictor of protection. Whereas most mAbs that protected to $\geq 60\%$ also showed a minimal unneutralized fraction (Figure 7C, upper right quadrant), others do not. VIC 143, VIC 145, and VIC 151 each had high protection levels despite leaving 100% (VIC 143, VIC 145) or 85% (VIC 151) of rVSV un-neutralized. Meanwhile, PF appears to be largely independent of neutralization activity (Figure 7D). Together, these statistical analyses show how multiple mAb features contribute to protection and can guide design of protective mAb cocktails.

DISCUSSION

The VIC study analyzed mAbs donated from laboratories around the world and identified from a variety of sources to gain greater insight into which antibody features confer protection and which assays best identify these features. This study also represents a

major effort to determine the level of agreement among neutralization assays and whether surrogate systems can substitute for authentic virus in these assays.

Considering the entire VIC panel, human EBOV mAbs were significantly more likely to protect than murine mAbs (43 human/49 highly protective). However, human mAbs in this study were typically chosen from larger panels in studies performed during or after the 2013–2016 epidemic. Therefore, we cannot rule out that the apparent improvement in protection simply reflects a greater selection stringency for these mAbs.

A unique feature of the VIC study was the casting of a broad and agnostic experimental net: each mAb was evaluated in each of 30 assays. Network correlation and machine learning approaches showed that among the features assessed, neutralization had the strongest correlation with protection ($\rho = 0.61$ – 0.68). Interestingly, however, among the 49 highly protective antibodies, only 20 had strong activity in all three neutralization assays while 29 did not, indicating that no single neutralization assay alone can always predict protection. K-means clustering

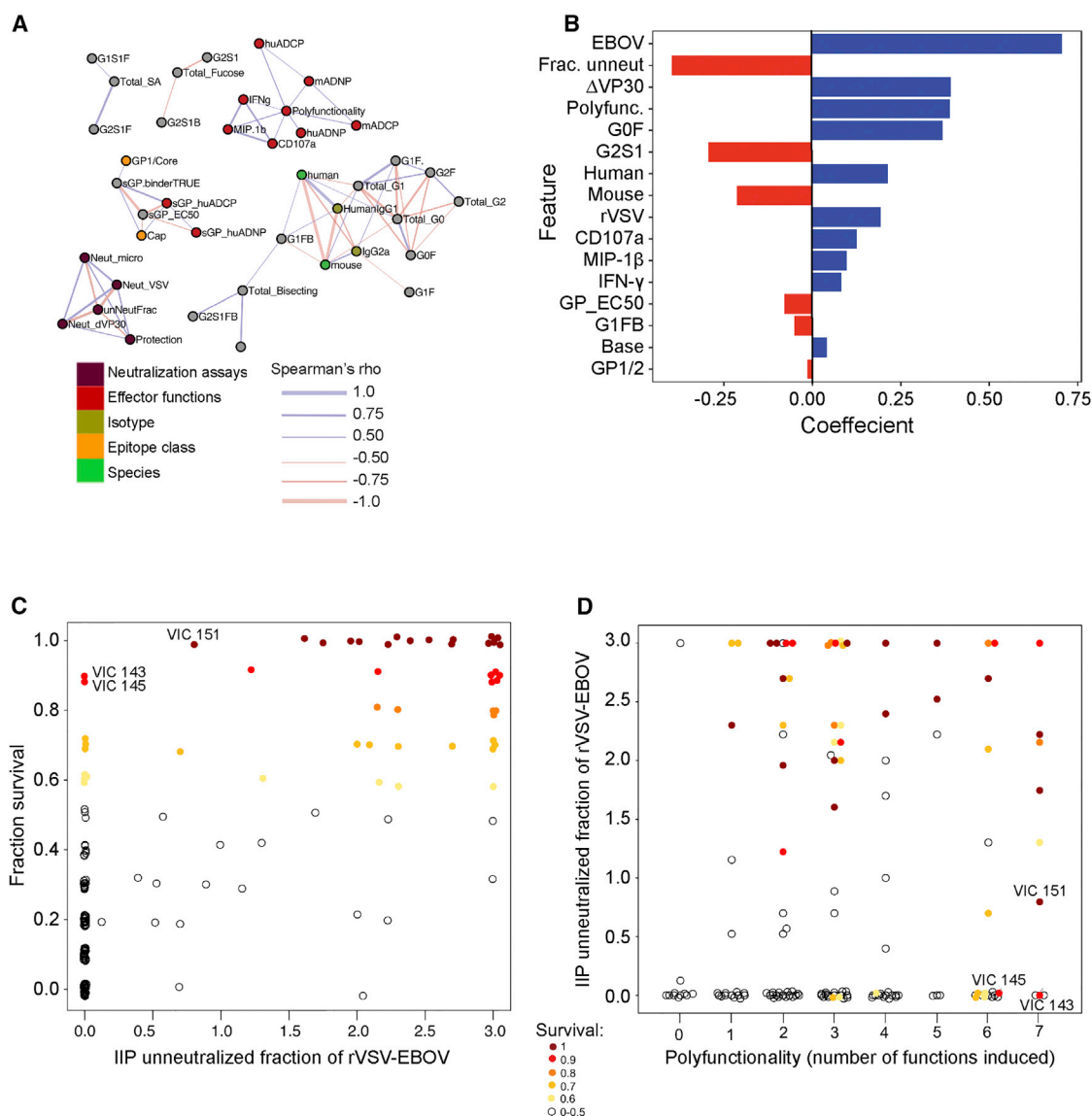


Figure 7. Network Analysis of Correlations between mAb Features

(A) Force directed network of statistically significant pairwise Spearman's rho correlation coefficients > 0.5 (positive, blue; negative, red). Colored nodes represent mAb features and line thickness corresponds to coefficient values.

(B) Coefficients of selected features in the logistic regression model with elastic net regularization calculated by:

$$P(\text{Protection} = \text{High}) = \frac{1}{1 + e^{-(\beta_0 + \beta_1 X_1 + \beta_2 X_2 + \beta_3 X_3 + \dots)}}$$

where P is probability and β is the coefficient that weights individual (X_i) features. Positive and negative coefficients imply that an increase in the value of the feature will increase and decrease, respectively, the probability of the mAb conferring "High" protection.

(C) Fraction of surviving mice plotted as a function of rVSV instantaneous inhibitory potential (IIP). Circles indicating individual mAbs are colored according to protection offered.

(D) rVSV IIP as a function of polyfunctionality. mAbs having high polyfunctionality but low (VIC 151) or no (VIC 143, VIC 145) rVSV neutralization are labeled.

indicated that the Δ VSP30 and rVSV assays tended to give a binary readout (i.e., yes/no), whereas authentic EBOV readouts captured a broader range of neutralization behavior (Figures 2 and 4). Further, each cluster contains mAbs from a variety of epitope classes, suggesting that epitope is not the sole determinant of neutralization behavior. However, three trends emerged:

Base and fusion loop mAbs were predominantly in cluster 5 (consistent neutralization in all systems); Most GP1/Core mAbs were cluster 1 (no neutralization in any system); and Glycan cap/sGP epitope mAbs were in all five clusters, but 11/21 were in Cluster 3 (antibodies that neutralized only in EBOV). We note several differences among the assays that could affect

neutralization readout including: (1) a shorter, bullet-shaped rhabdovirus particle in rVSV versus a longer, filovirion-shaped particle in Δ VP30 and authentic EBOV; (2) presence of wild-type sGP levels in Δ VP30 and EBOV assays versus no sGP in rVSV; and (3) detection of infected cells via reporter gene expression in rVSV and Δ VP30 versus KZ52-mediated detection of infected cells in authentic EBOV. Overall, the Δ VP30 assay was more stringent, focusing on the most potent neutralization hits, whereas the authentic EBOV assay was more forgiving, detecting a range of intermediate neutralization behavior and unique neutralizers (Figures 2A and 2E). Although the neutralization assays differed according to defined thresholds, absolute differences among the assays were clear (100% neutralization versus 0% neutralization) even at the highest antibody concentration (e.g., VIC 12, VIC 20, VIC 67), which cannot be explained by the chosen threshold alone.

Our results indicated that sGP cross-reactivity did not impede neutralization in assays where sGP was present. In some cases, neutralization activity was higher in the presence of sGP. Others found parallel results. For example, the sGP-reactive mAb BDBV289 neutralizes better than many mAbs against overlapping epitopes that lack sGP reactivity (Flyak et al., 2016). However, in another study, sGP competed for anti-GP antibodies, but only in mice immunized with sGP (Mohan et al., 2012).

mAbs recognizing GP_{CL} consistently neutralized. Among GP_{CL}-reactive epitopes, 8/8 HR2, 13/14 base, 7/8 fusion loop, and 5/6 of GP1/Head neutralized rVSV compared to 13/43 glycan cap and 0/20 mucin-directed mAbs (21/43 glycan cap and 1/20 mucin mAbs neutralized authentic EBOV). Further, mAbs against GP1/Core, GP1/2 and unassigned epitopes typically did not neutralize well. The inability to achieve a stable EM reconstruction or to obtain clear results by alanine scanning may be related to poor binding, which could also negatively affect neutralization.

IEFs also link to a spatial pattern on GP related to the distance from the viral membrane (Figure 6). Tier 1 mAbs consistently recruited higher phagocytic activity and in turn achieve greater levels of PF than Tiers 2 and 3 mAbs ($p = 0.31$ for Tier 1 versus $p < 0.1$, Tiers 2 and 3). An upper and outer antibody binding position on GP could assist Fc recognition by FcR-bearing cells (Lux et al., 2013). Influenza Fc behaves differently: stalk rather than head antibodies were noted to more successfully recruit Fc-mediated functions (Krammer and Palese, 2015).

The GP1/Head class had both high neutralization and IEF activity. Nearly all (5/6) GP1/Head antibodies were highly protective. mAb 114, a head-binding antibody not included in the panel, protects NHPs as a monotherapy (Corti et al., 2016). GP1/Head mAbs are consistently effective, but every epitope class included at least one highly protective mAb in mice.

Although neutralization correlated with protection, eight mAbs were protective in mice, yet failed to neutralize well. Of these, VIC 115 (GP1/Core), 121 (unknown) and 143 (mucin) lacked any neutralization activity, whereas VIC 137, 141, 145, and 152 (cap) and VIC 150 (GP1/Core) registered as moderate neutralizers only for authentic EBOV (Cluster 3). In total, five of these eight mAbs recognized Tier 1 epitopes. All eight recruited higher levels of IEF (mean PF, phagocytosis and NK function scores of 5.5/7, 3.4/4 and 2.25/3, respectively). In contrast, the nine

antibodies that neutralized well, but failed to protect $\geq 60\%$ (VIC 8, 11, 15, 16, 39, 42, 76, 83, and 101) had lower mean PF, phagocytosis, and NK function scores (2.5/7, 2.1/4 and 0.4/3, respectively).

Protective, but non- or weakly neutralizing mAbs constituted 5% of the VIC panel. More such antibodies could exist for Ebola virus, but may not have been pursued because initial antibody downselection is typically based on neutralization. In many EBOV vaccine studies, total antibody binding, rather than neutralization, is the best correlate of protection (Lennemann et al., 2017; Pushko et al., 2000; Schmaljohn and Lewis, 2016; Sullivan et al., 2009; Wong et al., 2012). Antibodies that recognize the IEF-linked, more accessible Tier 1 epitopes may even take precedence in polyclonal responses elicited by vaccination. Indeed, GP1/Head and glycan cap mAbs were the most abundantly recognized epitopes by antibodies in vaccinee sera (Khurana et al., 2016) after the first dose of rVSV-based EBOV vaccine (Regules et al., 2017). The frequency of these antibodies persisted after the second vaccine dose, whereas that of HR2 and membrane-proximal antibodies decreased.

Other recent studies illuminated the role of binding, but non-neutralizing, antibodies in mediating protection against other viruses (Bootz et al., 2017; Henry Dunand et al., 2016; Horwitz et al., 2017; Lewis et al., 2017; Mayr et al., 2017; Perez et al., 2017; Schmaljohn, 2013). Such antibodies may have contributed to the benefit observed in the RV144 HIV-1 vaccine trial (Corey et al., 2015; Santra et al., 2015) and provide added protection to that afforded by neutralizing antibodies, or when neutralizing antibodies are difficult to elicit.

One limitation of this study is the use of only Vero cells for the neutralization assays. Use of Vero cells links our results to previous studies, but numerous cell types would be infected *in vivo*. For *in vivo* protection assays, the large scale and study design (i.e., each mAb evaluated for *in vivo* protection) necessitated use of mice rather than NHPs. Moreover, for *in vivo* protection studies we evaluated only a single virus dose—the same dose used in earlier work—to allow comparisons across studies. On the other hand, the scale was perhaps not large enough: analysis of thousands of mAbs might be required for statistical significance in all comparisons and to dissect co-occurring variables such as glycan identity, FcR-mediated functions, and isotype. Our focus on IgG class mAbs that recognize Ebola virus GP and on post-exposure protection is an additional limitation. Certainly, in natural infection, IgM and IgA contribute to protection (Hasegawa et al., 2015), and antibodies against other viral antigens may contribute to recognition and killing of infected cells. Antibody stoichiometry, whether different antibody features or antibody classes would be required pre- rather than post-exposure, and how the array of desired antibodies elicited by vaccination might differ from mAbs are also unknown. Overall however, this study provides an array of biochemical, biophysical, and cellular assay data from which smaller, representative groups of mAbs could then be evaluated in larger animals (e.g., guinea pigs, ferrets, NHPs). Moving these representative groups forward would allow better comparison of protection, and understanding of what features drive protection, across commonly

used animal models. This dataset now provides a basis for selecting focused groups for precise engineering, alteration, and testing of single variables.

In summary, the major findings are: (1) both neutralization and immune PF contribute to *in vivo* protection; (2) mAbs recognizing regions retained in GP_{CL} were more likely to neutralize, whereas mAbs targeting upper Tier 1 epitopes were more likely to elicit phagocytosis; (3) neutralization assays yielded variable results, and disagreed about as often as they agreed, with discordance occurring primarily for mAbs with a significant un-neutralized fraction or those against the glycan cap; (4) the fusion loop, GP1/Head, and GP1/Core epitope groups had the highest frequency of ebolavirus cross-reactivity; (5) sGP reactivity did not influence neutralization or protection; (6) particular glycan structures could be positively or negatively correlated with protection, neutralization and IEF; and (7) network correlation and IIP calculation indicate that multiple factors are together predictive of mAb protection. Findings from this study can serve as a framework for future exploration, and for analysis of antibodies against other important human pathogens.

STAR METHODS

Detailed methods are provided in the online version of this paper and include the following:

- **KEY RESOURCES TABLE**
- **CONTACT FOR REAGENT AND RESOURCE SHARING**
- **EXPERIMENTAL MODEL AND SUBJECT DETAILS**
 - Monoclonal antibody isolation and purification
 - Mice
 - Cell lines
 - Primary cells
 - Viruses
- **METHOD DETAILS**
 - Expression and Purification of EBOV, Makona variant, BDBV, SUDV, RESTV and Marburg RAVN GPs
 - ELISA analysis of antibody binding to GP
 - Epitope mapping by electron microscopy of IgG Fab fragments complexed with GPΔTM
 - Epitope mapping by alanine scanning mutagenesis
 - Neutralization of EbolaΔVP30-RenLuc virus
 - Neutralization of authentic EBOV
 - Neutralization of rVSV-EBOV GP
 - Antibody-mediated protection of mice challenged with mouse-adapted EBOV
 - Immune effector assays
 - Antibody-mediated neutrophil phagocytosis (huADNP and mADNP)
 - Antibody-mediated NK cell degranulation and activation
 - Determination of polyfunctionality
 - Classification of functional activity into high, moderate, and low
 - Analysis of antibody glycan content
- **QUANTIFICATION AND STATISTICAL ANALYSES**
 - Machine learning and statistical analyses

SUPPLEMENTAL INFORMATION

Supplemental Information includes seven figures and four tables and can be found with this article online at <https://doi.org/10.1016/j.cell.2018.07.033>.

ACKNOWLEDGMENTS

The major support for this project was U19 AI109762, a Centers of Excellence in Translational Research Award of NIAID. We thank the over 200 individuals who contributed their time, reagents and expertise. We also thank Julius Lutwama (UVRI), Leslie Lobel (Ben Gurion), Robert Garry and James Robinson (Tulane), Frederick Holtsberg (IBT), Luis Branco (Zalgen), Armand Sprecher (MSF), Lisa Hensley (NIAID IRF), and Heinz Feldmann (NIAID RML) for valuable discussions. This is manuscript #29635 of TSRI. Alanine scanning was done under NIAID contract HHSN272201400058C to B.J.D.; C.I.W. was supported by Human Therapeutic Monoclonal Antibodies Platform IAF311007; K.G.A. acknowledges additional support from NIAID U19AI135995.

AUTHOR CONTRIBUTIONS

Conceptualization, E.O.S., G.P.K., Y.K., K.C., J.M.D.; Validation, E.O.S., S.L.S., K.G., Y.K., K.C., J.M.D., X.Q., G.P.K., K.W., B.K.; Formal Analysis, E.O.S., M.L.F., K.G., S.L.S., J.M.B., A.S.H., P.J.H., A.Z.W., B.M.G., X.Q., C.D.M., K.W., E.E.G., J.T., A.B.W., K.G.A., G.A.; Investigation, M.L.F., J.M.B., A.S.H., K.W., P.J.H., A.Z.W., B.M.G., S.H., X.Q., K.B.J.P., H.L.T., C.D.M., J.P., E.D.; T.B.K.; Resources, E.O.S., X.Q., R.A., M.J.A., A.B., D.R.B., J.E.C., C.W.D., G.G., F.K., C.A.K., J.R.L., C.N., M.H.P., P.R., A.T., A.R.T., V.V., L.M.W., C.I.W., L.Z., B.J.D., A.B.W., B.K., G.P.K., Y.K., G.A., K.C., J.M.D.; Data Curation, M.L.F., S.L.S.; Writing- Original Draft, E.O.S., Review & Editing, E.O.S., S.L.S.; Visualization, S.L.S., K.G., J.M.B., A.Z.W., B.M.G., C.D.M., K.W., E.O.S.; Funding Acquisition, E.O.S., G.P.K., Y.K., K.C., J.M.D.

DECLARATION OF INTERESTS

L.M.W. is an employee and shareholder of Adimab. C.N. is an employee of Emergent BioSolutions. M.J.A. is an employee of Integrated BioTherapeutics. E.D. and B.J.D. are employees of Integral Molecular and B.J.D. is a shareholder. M.H.P. is an employee of Mapp Biopharmaceutical and L.Z. is a shareholder and owner. C.A.K. is an employee of Regeneron.

Received: February 2, 2018

Revised: May 22, 2018

Accepted: July 24, 2018

Published: August 9, 2018

REFERENCES

- Ackerman, M.E., Mikhailova, A., Brown, E.P., Dowell, K.G., Walker, B.D., Bailey-Kellogg, C., Suscovich, T.J., and Alter, G. (2016). Polyfunctional HIV-Specific Antibody Responses Are Associated with Spontaneous HIV Control. *PLoS Pathog.* 12, e1005315.
- Alter, G., Malenfant, J.M., and Altfeld, M. (2004). CD107a as a functional marker for the identification of natural killer cell activity. *J. Immunol. Methods* 294, 15–22.
- Audet, J., Wong, G., Wang, H., Lu, G., Gao, G.F., Kobinger, G., and Qiu, X. (2014). Molecular characterization of the monoclonal antibodies composing ZMAb: a protective cocktail against Ebola virus. *Sci. Rep.* 4, 6881.
- Bootz, A., Karbach, A., Spindler, J., Kropff, B., Reuter, N., Sticht, H., Winkler, T.H., Britt, W.J., and Mach, M. (2017). Protective capacity of neutralizing and non-neutralizing antibodies against glycoprotein B of cytomegalovirus. *PLoS Pathog.* 13, e1006601.
- Bornholdt, Z.A., Turner, H.L., Murin, C.D., Li, W., Sok, D., Souders, C.A., Piper, A.E., Goff, A., Shamblin, J.D., Wollen, S.E., et al. (2016). Isolation of potent neutralizing antibodies from a survivor of the 2014 Ebola virus outbreak. *Science* 351, 1078–1083.

- Bray, M., Davis, K., Geisbert, T., Schmaljohn, C., and Huggins, J. (1998). A mouse model for evaluation of prophylaxis and therapy of Ebola hemorrhagic fever. *J. Infect. Dis.* 178, 651–661.
- Breiman, L. (2001). Random Forests. *Mach. Learn.* 45, 5–32.
- Bruhns, P. (2012). Properties of mouse and human IgG receptors and their contribution to disease models. *Blood* 119, 5640–5649.
- Chandran, K., Sullivan, N.J., Felbor, U., Whelan, S.P., and Cunningham, J.M. (2005). Endosomal proteolysis of the Ebola virus glycoprotein is necessary for infection. *Science* 308, 1643–1645.
- Chung, A.W., Ghebremichael, M., Robinson, H., Brown, E., Choi, I., Lane, S., Dugast, A.-S., Schoen, M.K., Rolland, M., Suscovich, T.J., et al. (2014). Polyfunctional Fc-effector profiles mediated by IgG subclass selection distinguish RV144 and VAX003 vaccines. *Sci. Transl. Med.* 6, 228ra38.
- Corey, L., Gilbert, P.B., Tomaras, G.D., Haynes, B.F., Pantaleo, G., and Fauci, A.S. (2015). Immune correlates of vaccine protection against HIV-1 acquisition. *Sci. Transl. Med.* 7, 310rv7.
- Corti, D., Misasi, J., Mulangu, S., Stanley, D.A., Kanekiyo, M., Wollen, S., Ploquin, A., Doria-Rose, N.A., Staupé, R.P., Bailey, M., et al. (2016). Protective monotherapy against lethal Ebola virus infection by a potentially neutralizing antibody. *Science* 351, 1339–1342.
- Davidson, E., Bryan, C., Fong, R.H., Barnes, T., Pfaff, J.M., Mabila, M., Rucker, J.B., and Doranz, B.J. (2015). Mechanism of Binding to Ebola Virus Glycoprotein by the ZMapp, ZMAb, and MB-003 Cocktail Antibodies. *J. Virol.* 89, 10982–10992.
- Dias, J.M., Kuehne, A.I., Abelson, D.M., Bale, S., Wong, A.C., Halfmann, P., Muhammad, M.A., Fusco, M.L., Zak, S.E., Kang, E., et al. (2011). A shared structural solution for neutralizing ebolaviruses. *Nat. Struct. Mol. Biol.* 18, 1424–1427.
- Dube, D., Brecher, M.B., Delos, S.E., Rose, S.C., Park, E.W., Schornberg, K.L., Kuhn, J.H., and White, J.M. (2009). The primed ebolavirus glycoprotein (19-kilodalton GP1,2): sequence and residues critical for host cell binding. *J. Virol.* 83, 2883–2891.
- Ebihara, H., Takada, A., Kobasa, D., Jones, S., Neumann, G., Theriault, S., Bray, M., Feldmann, H., and Kawaoka, Y. (2006). Molecular determinants of Ebola virus virulence in mice. *PLoS Pathog.* 2, e73–e73.
- Ewer, K., Rampling, T., Venkatraman, N., Bowyer, G., Wright, D., Lambe, T., Imoukhuede, E.B., Payne, R., Fehling, S.K., Strecker, T., et al. (2016). A Monovalent Chimpanzee Adenovirus Ebola Vaccine Boosted with MVA. *N. Engl. J. Med.* 374, 1635–1646.
- Flyak, A.I., Illykh, P.A., Murin, C.D., Garron, T., Shen, X., Fusco, M.L., Hashiguchi, T., Bornholdt, Z.A., Slaughter, J.C., Sappapapu, G., et al. (2015). Mechanism of human antibody-mediated neutralization of Marburg virus. *Cell* 160, 893–903.
- Flyak, A.I., Shen, X., Murin, C.D., Turner, H.L., David, J.A., Fusco, M.L., Lampley, R., Kose, N., Illykh, P.A., Kuzmina, N., et al. (2016). Cross-Reactive and Potent Neutralizing Antibody Responses in Human Survivors of Natural Ebola virus Infection. *Cell* 164, 392–405.
- Fusco, M.L., Hashiguchi, T., Cassan, R., Biggins, J.E., Murin, C.D., Warfield, K.L., Li, S., Holtsberg, F.W., Shulenin, S., Vu, H., et al. (2015). Protective mAbs and Cross-Reactive mAbs Raised by Immunization with Engineered Marburg Virus GPs. *PLoS Pathog.* 11, e1005016.
- Geurts, P., Ernst, D., and Wehenkel, L. (2006). Extremely randomized trees. *Mach. Learn.* 63, 3–42.
- Gibb, T.R., Bray, M., Geisbert, T.W., Steele, K.E., Kell, W.M., Davis, K.J., and Jaax, N.K. (2001). Pathogenesis of experimental Ebola Zaire virus infection in BALB/c mice. *J. Comp. Pathol.* 125, 233–242.
- Goh, A.X.H., Bertin-Maghit, S., Ping Yeo, S., Ho, A.W.S., Derks, H., Mortellaro, A., and Wang, C.-I. (2014). A novel human anti-interleukin-1 β neutralizing monoclonal antibody showing *in vivo* efficacy. *MAbs* 6, 765–773.
- Gunn, B.M., Yu, W.-H., Karim, M.M., Brannan, J., Wec, A.Z., Fusco, M.L., Schendel, S.L., Gangavarapu, K., Das, J., Suscovich, T., et al. (2018). Dissecting the role of Fc and Fab mediated functions in Ebola virus specific immunity. *Cell Host Microbe*. <https://doi.org/10.1016/j.chom.2018.07.015>.
- Halfmann, P., Kim, J.H., Ebihara, H., Noda, T., Neumann, G., Feldmann, H., and Kawaoka, Y. (2008). Generation of biologically contained Ebola viruses. *Proc. Natl. Acad. Sci. USA* 105, 1129–1133.
- Hasegawa, H., van Reijt, E., and Kida, H. (2015). Mucosal immunization and adjuvants. *Curr. Top. Microbiol. Immunol.* 386, 371–380.
- Hashiguchi, T., Fusco, M.L., Bornholdt, Z.A., Lee, J.E., Flyak, A.I., Matsuo, R., Kohda, D., Yanagi, Y., Hammel, M., Crowe, J.E., Jr., and Saphire, E.O. (2015). Structural basis for Marburg virus neutralization by a cross-reactive human antibody. *Cell* 160, 904–912.
- Haynes, B.F., Gilbert, P.B., McElrath, M.J., Zolla-Pazner, S., Tomaras, G.D., Alam, S.M., Evans, D.T., Montefiori, D.C., Karnasuta, C., Sutthent, R., et al. (2012). Immune-correlates analysis of an HIV-1 vaccine efficacy trial. *N. Engl. J. Med.* 366, 1275–1286.
- Henry Dunand, C.J., Leon, P.E., Huang, M., Choi, A., Chromikova, V., Ho, I.Y., Tan, G.S., Cruz, J., Hirsh, A., Zheng, N.-Y., et al. (2016). Both Neutralizing and Non-Neutralizing Human H7N9 Influenza Vaccine-Induced Monoclonal Antibodies Confer Protection. *Cell Host Microbe* 19, 800–813.
- Holtsberg, F.W., Shulenin, S., Vu, H., Howell, K.A., Patel, S.J., Gunn, B., Karim, M., Lai, J.R., Frei, J.C., Nyakatura, E.K., et al. (2015). Pan-ebolavirus and Pan-filovirus Mouse Monoclonal Antibodies: Protection against Ebola and Sudan Viruses. *J. Virol.* 90, 266–278.
- Horwitz, J.A., Bar-On, Y., Lu, C.-L., Fera, D., Lockhart, A.A.K., Lorenzi, J.C.C., Nogueira, L., Golijanin, J., Scheid, J.F., Seaman, M.S., et al. (2017). Non-neutralizing Antibodies Alter the Course of HIV-1 Infection *In Vivo*. *Cell* 170, 637–648.e10.
- Huang, K.-Y.A., Rijal, P., Schimanski, L., Powell, T.J., Lin, T.-Y., McCauley, J.W., Daniels, R.S., and Townsend, A.R. (2015). Focused antibody response to influenza linked to antigenic drift. *J. Clin. Invest.* 125, 2631–2645.
- Illykh, P.A., Shen, X., Flyak, A.I., Kuzmina, N., Ksiazek, T.G., Crowe, J.E., Jr., and Bukreyev, A. (2016). Chimeric Filoviruses for Identification and Characterization of Monoclonal Antibodies. *J. Virol.* 90, 3890–3901.
- Keck, Z.-Y., Enterlein, S.G., Howell, K.A., Vu, H., Shulenin, S., Warfield, K.L., Froude, J.W., Araghi, N., Douglas, R., Biggins, J., et al. (2015). Macaque Monoclonal Antibodies Targeting Novel Conserved Epitopes within Filovirus Glycoprotein. *J. Virol.* 90, 279–291.
- Khurana, S., Fuentes, S., Coyle, E.M., Ravichandran, S., Davey, R.T., Jr., and Beigel, J.H. (2016). Human antibody repertoire after VSV-Ebola vaccination identifies novel targets and virus-neutralizing IgM antibodies. *Nat. Med.* 22, 1439–1447.
- Koellhoffer, J.F., Chen, G., Sandesara, R.G., Bale, S., Saphire, E.O., Chandran, K., Sidhu, S.S., and Lai, J.R. (2012). Two synthetic antibodies that recognize and neutralize distinct proteolytic forms of the ebola virus envelope glycoprotein. *ChemBioChem* 13, 2549–2557.
- Krammer, F., and Palese, P. (2015). Advances in the development of influenza virus vaccines. *Nat. Rev. Drug Discov.* 14, 167–182.
- Lee, J.E., Fusco, M.L., Hessel, A.J., Oswald, W.B., Burton, D.R., and Saphire, E.O. (2008). Structure of the Ebola virus glycoprotein bound to an antibody from a human survivor. *Nature* 454, 177–182.
- Lenemann, N.J., Herbert, A.S., Brouillette, R., Rhein, B., Bakken, R.A., Perschbacher, K.J., Cooney, A.L., Miller-Hunt, C.L., Ten Eyck, P., Biggins, J., et al. (2017). Vesicular stomatitis virus pseudotyped with Ebola virus glycoprotein serves as a protective, non-infectious vaccine against Ebola virus challenge in mice. *J. Virol.* 91, e00479-17.
- Lewis, G.K., Finzi, A., DeVico, A.L., and Pazgier, M. (2015). Conformational Masking and Receptor-Dependent Unmasking of Highly Conserved Env Epitopes Recognized by Non-Neutralizing Antibodies That Mediate Potent ADCC against HIV-1. *Viruses* 7, 5115–5132.
- Lewis, G.K., Pazgier, M., Evans, D.T., Ferrari, G., Bournazos, S., Parsons, M.S., Bernard, N.F., and Finzi, A. (2017). Beyond Viral Neutralization. *AIDS Res. Hum. Retroviruses* 33, 760–764.
- Li, D., Chen, T., Hu, Y., Zhou, Y., Liu, Q., Zhou, D., Jin, X., and Huang, Z. (2016). An Ebola Virus-Like Particle-Based Reporter System Enables Evaluation of

- Antiviral Drugs *In Vivo* under Non-Biosafety Level 4 Conditions. *J. Virol.* **90**, 8720–8728.
- Lux, A., Yu, X., Scanlan, C.N., and Nimmerjahn, F. (2013). Impact of immune complex size and glycosylation on IgG binding to human FcγRs. *J. Immunol.* **190**, 4315–4323.
- Macdonald, L.E., Karow, M., Stevens, S., Auerbach, W., Poueymirou, W.T., Yasenchak, J., Frendewey, D., Valenzuela, D.M., Giallourakis, C.C., Alt, F.W., et al. (2014). Precise and *in situ* genetic humanization of 6 Mb of mouse immunoglobulin genes. *Proc. Natl. Acad. Sci. USA* **111**, 5147–5152.
- Mahan, A.E., Tedesco, J., Dionne, K., Baruah, K., Cheng, H.D., De Jager, P.L., Barouch, D.H., Suscovich, T., Ackerman, M., Crispin, M., and Alter, G. (2015). A method for high-throughput, sensitive analysis of IgG Fc and Fab glycosylation by capillary electrophoresis. *J. Immunol. Methods* **417**, 34–44.
- Maruyama, T., Rodriguez, L.L., Jahrling, P.B., Sanchez, A., Khan, A.S., Nichol, S.T., Peters, C.J., Parren, P.W., and Burton, D.R. (1999). Ebola virus can be effectively neutralized by antibody produced in natural human infection. *J. Virol.* **73**, 6024–6030.
- Marzi, A., Yoshida, R., Miyamoto, H., Ishijima, M., Suzuki, Y., Higuchi, M., Matsuyama, Y., Igarashi, M., Nakayama, E., Kuroda, M., et al. (2012). Protective efficacy of neutralizing monoclonal antibodies in a nonhuman primate model of Ebola hemorrhagic fever. *PLoS ONE* **7**, e36192.
- Mayr, L.M., Decoville, T., Schmidt, S., Laumond, G., Klingler, J., Ducloy, C., Bahram, S., Zolla-Pazner, S., and Moog, C. (2017). Non-neutralizing Antibodies Targeting the V1V2 Domain of HIV Exhibit Strong Antibody-Dependent Cell-mediated Cytotoxic Activity. *Sci. Rep.* **7**, 12655.
- Miller, E.H., Obernosterer, G., Raaben, M., Herbert, A.S., Deffieu, M.S., Krishnan, A., Ndungo, E., Sandesara, R.G., Carette, J.E., Kuehne, A.I., et al. (2012). Ebola virus entry requires the host-programmed recognition of an intracellular receptor. *EMBO J.* **31**, 1947–1960.
- Mohan, G.S., Li, W., Ye, L., Compans, R.W., and Yang, C. (2012). Antigenic subversion: a novel mechanism of host immune evasion by Ebola virus. *PLoS Pathog.* **8**, e1003065.
- Murin, C.D., Fusco, M.L., Bornholdt, Z.A., Qiu, X., Olinger, G.G., Zeitlin, L., Kobinger, G.P., Ward, A.B., and Saphire, E.O. (2014). Structures of protective antibodies reveal sites of vulnerability on Ebola virus. *Proc. Natl. Acad. Sci. USA* **111**, 17182–17187.
- Murphy, A.J., Macdonald, L.E., Stevens, S., Karow, M., Dore, A.T., Pobursky, K., Huang, T.T., Poueymirou, W.T., Esau, L., Meola, M., et al. (2014). Mice with megabase humanization of their immunoglobulin genes generate antibodies as efficiently as normal mice. *Proc. Natl. Acad. Sci. USA* **111**, 5153–5158.
- Olinger, G.G., Jr., Pettitt, J., Kim, D., Working, C., Bohorov, O., Bratcher, B., Hiatt, E., Hume, S.D., Johnson, A.K., Morton, J., et al. (2012). Delayed treatment of Ebola virus infection with plant-derived monoclonal antibodies provides protection in rhesus macaques. *Proc. Natl. Acad. Sci. USA* **109**, 18030–18035.
- Oliva, A., Kinter, A.L., Vaccarezza, M., Rubbert, A., Catanzaro, A., Moir, S., Monaco, J., Ehler, L., Mizell, S., Jackson, R., et al. (1998). Natural killer cells from human immunodeficiency virus (HIV)-infected individuals are an important source of CC-chemokines and suppress HIV-1 entry and replication *in vitro*. *J. Clin. Invest.* **102**, 223–231.
- Oswald, W.B., Geisbert, T.W., Davis, K.J., Geisbert, J.B., Sullivan, N.J., Jahrling, P.B., Parren, P.W.H.I., and Burton, D.R. (2007). Neutralizing antibody fails to impact the course of Ebola virus infection in monkeys. *PLoS Pathog.* **3**, e9.
- Pascal, K.E., Dudgeon, D., Trefry, J.C., Anantpadma, M., Sakurai, Y., Murin, C.D., Turner, H.L., Fairhurst, J., Torres, M., Rafique, A., et al. (2018). Development of clinical-stage human monoclonal antibodies that treat advanced Ebola virus disease in non-human primates. *J. Infect. Dis.* <https://doi.org/10.1093/infdis/jiy285>.
- Pedregosa, F., Varoquaux, G., Gramfort, A., Michel, V., Thirion, B., Grisel, O., Blondel, M., Prettenhofer, P., Weiss, R., Dubourg, V., et al. (2011). Scikit-learn: Machine Learning in Python. *J. Mach. Learn. Res.* **12**, 2825–2830.
- Perez, L.G., Martinez, D.R., deCamp, A.C., Pinter, A., Berman, P.W., Francis, D., Sinangil, F., Lee, C., Greene, K., Gao, H., et al. (2017). V1V2-specific complement activating serum IgG as a correlate of reduced HIV-1 infection risk in RV144. *PLoS ONE* **12**, e0180720.
- Pettersen, E.F., Goddard, T.D., Huang, C.C., Couch, G.S., Greenblatt, D.M., Meng, E.C., and Ferrin, T.E. (2004). UCSF Chimera—a visualization system for exploratory research and analysis. *J. Comput. Chem.* **25**, 1605–1612.
- Pushko, P., Bray, M., Ludwig, G.V., Parker, M., Schmaljohn, A., Sanchez, A., Jahrling, P.B., and Smith, J.F. (2000). Recombinant RNA replicons derived from attenuated Venezuelan equine encephalitis virus protect guinea pigs and mice from Ebola hemorrhagic fever virus. *Vaccine* **19**, 142–153.
- Qiu, X., Alimonti, J.B., Melito, P.L., Fernando, L., Ströher, U., and Jones, S.M. (2011). Characterization of Zaire ebolavirus glycoprotein-specific monoclonal antibodies. *Clin. Immunol.* **141**, 218–227.
- Qiu, X., Fernando, L., Melito, P.L., Audet, J., Feldmann, H., Kobinger, G., Alimonti, J.B., and Jones, S.M. (2012). Ebola GP-specific monoclonal antibodies protect mice and guinea pigs from lethal Ebola virus infection. *PLoS Negl. Trop. Dis.* **6**, e1575.
- Qiu, X., Wong, G., Audet, J., Bello, A., Fernando, L., Alimonti, J.B., Fausther-Bovendo, H., Wei, H., Aviles, J., Hiatt, E., et al. (2014). Reversion of advanced Ebola virus disease in nonhuman primates with ZMapp. *Nature* **514**, 47–53.
- Regules, J.A., Beigel, J.H., Paolino, K.M., Voell, J., Castellano, A.R., Hu, Z., Muñoz, P., Moon, J.E., Ruck, R.C., Bennett, J.W., et al.; rVSVΔG-ZEBOV-GP Study Group (2017). A Recombinant Vesicular Stomatitis Virus Ebola Vaccine. *N. Engl. J. Med.* **376**, 330–341.
- Sanchez, A., Trappier, S.G., Mahy, B.W., Peters, C.J., and Nichol, S.T. (1996). The virion glycoproteins of Ebola viruses are encoded in two reading frames and are expressed through transcriptional editing. *Proc. Natl. Acad. Sci. USA* **93**, 3602–3607.
- Sanchez, A., Yang, Z.Y., Xu, L., Nabel, G.J., Crews, T., and Peters, C.J. (1998). Biochemical analysis of the secreted and virion glycoproteins of Ebola virus. *J. Virol.* **72**, 6442–6447.
- Santra, S., Tomaras, G.D., Warrier, R., Nicely, N.I., Liao, H.-X., Pollara, J., Liu, P., Alam, S.M., Zhang, R., Cocklin, S.L., et al. (2015). Human Non-neutralizing HIV-1 Envelope Monoclonal Antibodies Limit the Number of Founder Viruses during SHIV Mucosal Infection in Rhesus Macaques. *PLoS Pathog.* **11**, e1005042.
- Saphire, E.O., Dye, J.M., Kobinger, G.P., Zeitlin, L., Chandran, K., and Garry, R.F. (2017). How to turn competitors into collaborators. *Nature* **541**, 283–285.
- Schmaljohn, A.L. (2013). Protective antiviral antibodies that lack neutralizing activity: precedents and evolution of concepts. *Curr. HIV Res.* **11**, 345–353.
- Schmaljohn, A., and Lewis, G.K. (2016). Cell-targeting antibodies in immunity to Ebola. *Pathog. Dis.* **74**, ftw021.
- Schornberg, K., Matsuyama, S., Kabsch, K., Delos, S., Bouton, A., and White, J. (2006). Role of endosomal cathepsins in entry mediated by the Ebola virus glycoprotein. *J. Virol.* **80**, 4174–4178.
- Shedlock, D.J., Bailey, M.A., Popernack, P.M., Cunningham, J.M., Burton, D.R., and Sullivan, N.J. (2010). Antibody-mediated neutralization of Ebola virus can occur by two distinct mechanisms. *Virology* **401**, 228–235.
- Shields, R.L., Lai, J., Keck, R., O'Connell, L.Y., Hong, K., Meng, Y.G., Weikert, S.H.A., and Presta, L.G. (2002). Lack of fucose on human IgG1 N-linked oligosaccharide improves binding to human FcγRIII and antibody-dependent cellular toxicity. *J. Biol. Chem.* **277**, 26733–26740.
- Smith, K., Garman, L., Wrammert, J., Zheng, N.-Y., Capra, J.D., Ahmed, R., and Wilson, P.C. (2009). Rapid generation of fully human monoclonal antibodies specific to a vaccinating antigen. *Nat. Protoc.* **4**, 372–384.
- Sullivan, N.J., Martin, J.E., Graham, B.S., and Nabel, G.J. (2009). Correlates of protective immunity for Ebola vaccines: implications for regulatory approval by the animal rule. *Nat. Rev. Microbiol.* **7**, 393–400.
- Takada, A., Feldmann, H., Stroher, U., Bray, M., Watanabe, S., Ito, H., McGregor, M., and Kawaoka, Y. (2003). Identification of protective epitopes on ebola virus glycoprotein at the single amino acid level by using recombinant vesicular stomatitis viruses. *J. Virol.* **77**, 1069–1074.
- Volchkov, V.E., Becker, S., Volchkova, V.A., Ternovoj, V.A., Kotov, A.N., Nete-sov, S.V., and Klenk, H.D. (1995). GP mRNA of Ebola virus is edited by the

- Ebola virus polymerase and by T7 and vaccinia virus polymerases. *Virology* 214, 421–430.
- Waggoner, S.N., Reighard, S.D., Gyurova, I.E., Cranert, S.A., Mahl, S.E., Karnele, E.P., McNally, J.P., Moran, M.T., Brooks, T.R., Yaqoob, F., and Rydzynski, C.E. (2016). Roles of natural killer cells in antiviral immunity. *Curr. Opin. Virol.* 16, 15–23.
- Wec, A.Z., Nyakatura, E.K., Herbert, A.S., Howell, K.A., Holtsberg, F.W., Bakken, R.R., Mittler, E., Christin, J.R., Shulenin, S., Jangra, R.K., et al. (2016). A “Trojan horse” bispecific-antibody strategy for broad protection against ebolaviruses. *Science* 354, 350–354.
- Wilkinson, D.E., Page, M., Mattiuzzo, G., Hassall, M., Dougall, T., Rigsby, P., Stone, L., and Minor, P. (2017). Comparison of platform technologies for assaying antibody to Ebola virus. *Vaccine* 35, 1347–1352.
- Wilson, J.A., Hevey, M., Bakken, R., Guest, S., Bray, M., Schmaljohn, A.L., and Hart, M.K. (2000). Epitopes involved in antibody-mediated protection from Ebola virus. *Science* 287, 1664–1666.
- Wong, A.C., Sandesara, R.G., Mulherkar, N., Whelan, S.P., and Chandran, K. (2010). A forward genetic strategy reveals destabilizing mutations in the Ebolavirus glycoprotein that alter its protease dependence during cell entry. *J. Virol.* 84, 163–175.
- Wong, G., Richardson, J.S., Pillet, S., Patel, A., Qiu, X., Alimonti, J., Hogan, J., Zhang, Y., Takada, A., Feldmann, H., and Kobinger, G.P. (2012). Immune parameters correlate with protection against ebola virus infection in rodents and nonhuman primates. *Sci. Transl. Med.* 4, 158ra146.
- Zhao, X., Howell, K.A., He, S., Brannan, J.M., Wec, A.Z., Davidson, E., Turner, H.L., Chiang, C.-I., Lei, L., Fels, J.M., et al. (2017). Immunization-Elicited Broadly Protective Antibody Reveals Ebolavirus Fusion Loop as a Site of Vulnerability. *Cell* 169, 891–904.e15.
- Zou, H., and Hastie, T. (2005). Regularization and variable selection via the elastic net. *J. R. Stat. Soc. Series B Stat. Methodol.* 67, 301–320.

STAR METHODS

KEY RESOURCES TABLE

REAGENT or RESOURCE	SOURCE	IDENTIFIER
Antibodies		
2G4	Mapp Bio	N/A
4G7	Mapp Bio	N/A
Alexa Fluor 488 AffiniPure donkey anti-mouse IgG	Jackson ImmunoResearch Laboratories, Inc.	715-545-150; RIID:AB_2340846
Alexa Fluor 488 AffiniPure goat anti-human IgG	Jackson ImmunoResearch Laboratories, Inc.	109-545-006; RIID:AB_2337832
Anti-CD107a	BD Biosciences	555802; RIID:AB_396136
b12	Polymun	AB011
c13C6	Mapp Bio	N/A
Guinea pig complement	Cedarlane	CL4051
Goat anti-human IgG secondary antibody	Thermo Fisher Scientific	31413; RIID:AB_429693
Goat anti-mouse IgG secondary antibody	Thermo Fisher Scientific	31437; RIID:AB_228295
KZ52	Maruyama et al., 1999 , Lee et al., 2008	N/A
VIC Antibody set 1	Wilson et al., 2000	N/A
VIC Antibody set 2	Takada et al., 2003	N/A
VIC Antibody set 3	Qiu et al., 2011 ; Qiu et al., 2012	N/A
VIC Antibody set 4	Flyak et al., 2016	N/A
VIC Antibody set 5	Ewer et al., 2016 ; Huang et al., 2015	N/A
VIC Antibody set 6	Keck et al., 2015	N/A
VIC Antibody set 7	Goh et al., 2014	N/A
VIC Antibody set 8	Davis and Ahmed unpublished data; Smith et al., 2009	N/A
VIC Antibody set 9	Murphy et al., 2014 ; Macdonald et al., 2014 ; Pascal et al., 2018	N/A
VIC Antibody set 10	Wec et al., 2016 ; Bornholdt et al., 2016	N/A
Viruses		
EbolaΔVP30-RenLuc virus	Halfmann et al., 2008	N/A
Mouse-adapted EBOV/Mayinga (EBOV/M.mus-tc/COD/76/Yambuku-Mayinga)	Bray et al., 1998	N/A
rVSV-EBOV/Mayinga GP (EBOV/H.sap-tc/COD/76/Yambuku-Mayinga)	Wong et al., 2010	N/A
Chemicals, Peptides, and Recombinant Proteins		
9-aminopyrene-1,4,6-trisulfonic acid (APTS)	Life Technologies	A6257
Brefeldin A	Sigma Aldrich	B7651
EBOV GPΔMuc	Fusco et al., 2015	N/A
EBOV GPΔTM	IBT Biotherapeutics; Lee et al., 2008	0501-015/n/a
EBOV GPΔTM	Fusco et al., 2015	N/A
EBOV GPcl	Fusco et al., 2015	N/A
EBOV GPQ508R	Audet et al., 2014	N/A
EBOV sGP	Fusco et al., 2015	N/A
EnduRen	Promega	E6481
FabRICATOR IdeS	Genovis	A0-FR1-096
GolgiStop	BD Biosciences	554724
marburgvirus Ravn virus GP	Fusco et al., 2015	N/A

(Continued on next page)

Continued

REAGENT or RESOURCE	SOURCE	IDENTIFIER
PNGase F	New England Biolabs	P0704S
Step-Tactin resin	QIAGEN	30002
Streptavidin, Alex Fluor conjugate	Life Technologies	S11223
SuperScript III Reverse Transcriptase	Thermo Fisher Scientific	18080093
Critical Commercial Assays		
RosetteSep	Stem Cell Technologies	15025
TMB substrate kit	Pierce	34021
Experimental Models: Cell Lines		
<i>Drosophila</i> : Schneider 2	Thermo Fisher Scientific	R69007
Hamster: ExpiCHO-S	Thermo Fisher Scientific	A12933
Human: HEK293	ATCC	CRL-1573
Human: THP-1 monocytes	ATCC	TIB-202
Monkey: Vero E6	ATCC	CRL-1586
Monkey: Vero VP30	Halfmann et al., 2008	N/A
Mouse: RAW264.7 monocytes	ATCC	TIB-71
Experimental Models: Organisms/Strains		
Mouse: Female BALB/cAnNCrl	Charles River	Strain Code 028
Mouse: VelocImmune	Macdonald et al., 2014 ; Murphy et al., 2014	n/a
Recombinant DNA		
EBOV GPΔMuc	Goh et al., 2014	GenBank: KM233090
rEBOVGP33-308	Goh et al., 2014	GenBank: AAC54887.1
Software and Algorithms		
BD Diva software	BD Biosciences	N/A
ExtraTreesRegressor	Geurts et al., 2006	N/A
FlowJo software	BD Biosciences	N/A
GraphPad Prism 7	GraphPad Software, Inc.	N/A
Harmony software	Perkin-Elmer	N/A
Python scikit-learn package	Pedregosa et al., 2011	N/A
R	R Project for Statistical Computing	http://www.r-project.org
R Caret	R Project for Statistical Computing	https://cran.r-project.org/package=caret
Other		
3130 XL ABI DNA Sequencer with 36 cm capillary and POP7 polymer	Applied Biosystems	N/A
BD LSRII flow cytometer	BD Biosciences	N/A
CellInsight CX5 High Content Screening (HCS) Platform	Thermo Fisher Scientific	CX51110
Intellicyt flow cytometer	Davidson et al., 2015	N/A
Operetta High Content Imaging System	Perkin-Elmer	N/A
Superdex 200 Increase 10/300 GL column	GE Healthcare Sciences	28990944
Tecan M1000 plate reader	Tecan	N/A
Tecna Spirit electron microscope with TemCam F416 4k x 4k CCD	Zhao et al., 2017	N/A

CONTACT FOR REAGENT AND RESOURCE SHARING

Further information and requests for resources and reagents should be directed to and will be fulfilled by the Lead Contact, Erica Ollmann Saphire (erica@scripps.edu).

EXPERIMENTAL MODEL AND SUBJECT DETAILS

Monoclonal antibody isolation and purification

Monoclonal antibodies (mAbs) were donated in sets. Some sets were purified according to previously described methods (Bornholdt et al., 2016; Flyak et al., 2015, 2016 Fusco et al., 2015; Holtsberg et al., 2015; Keck et al., 2015; Qiu et al., 2011, 2014; Takada et al., 2003; Wilson et al., 2000). For one set of mAbs, VelocImmune® mice (Macdonald et al., 2014; Murphy et al., 2014) were immunized with purified EBOV GP as immunogens. Splenocytes were then harvested and used to isolate EBOV GP-reactive B cells. cDNAs from reactive B cells were synthesized via reverse transcriptase (RT) reaction (SuperScript III, Invitrogen) and the variable heavy and light chains were amplified by PCR and cloned into expression vectors containing a human IgG1 heavy chain constant region and kappa light chain constant region, respectively. Recombinant anti-EBOV GP antibodies were produced in CHO cells following stable transfection with paired expression plasmids carrying heavy and light chains derived from the same B cell. Antibodies were purified from culture supernatants by Protein A affinity chromatography. One set of antibodies was isolated from human volunteers primed with chimpanzee adenovirus expressing Zaire GP (ChAD3 EBO Z) and boosted with MVA-BN Filo (modified Vaccinia expressing Ebola, Sudan and Marburg virus GPs and Taï Forest virus NP) vaccines (Ewer et al., 2016). Antibodies were purified as described in Huang et al. (Huang et al., 2015). Another mAb set was derived using recombinant EBOVGPΔmucin (GenBank: KM233090) or two rounds of panning with EBOVGPΔmucin followed by two rounds of panning with rEBOVGP33-308 (GenBank: AAC54887.1) or EBOVGPΔmucin followed by one round of panning with rEBOVGP33-308. Antibody isolation using phage display technology was performed according to Goh et al. (Goh et al., 2014). For another set, antibody heavy and light chain variable region genes were cloned from peripheral blood B cells and plasmablasts of patients treated for Ebola virus disease at Emory University hospital (Davis and Ahmed, unpublished data). Antibodies were produced in HEK293 cells as human IgG1s as previously described (Smith et al., 2009).

Mice

Female BALB/c mice, aged 6 to 8 weeks-old (Charles River Laboratory) housed in microisolator cages and given chow and water *ad libitum* were used for *in vivo* protection assays. All animal work involving infectious live virus was performed in the BSL-4 laboratories at USAMRIID or PHAC. At USAMRIID, all work with animals was conducted in compliance with the Animal Welfare Act and other Federal statutes and regulations relating to animals and experiments involving animals and adhered to the principles stated in the Guide for the Care and Use of Laboratory Animals, NRC Publication, 1996 edition. All procedures were reviewed and approved by the appropriate Institutional Animal Care and Use Committee at USAMRIID. Work performed at PHAC was approved by the Canadian Science Centre for Human and Animal Health Animal Care Committee following the guidelines of the Canadian Council on Animal Care.

Cell lines

Drosophila Schneider 2 (S2) were used for purification of recombinant GPs. HEK293 and ExpiCHO cultured according to the manufacturer's instructions were used for mAb purification. HEK293T cells were used for alanine scanning mutagenesis. The ΔVP30 neutralization used Vero cells expressing Ebola virus VP30 that were cultured as previously described (Halfmann et al., 2008). *In vitro* neutralization assays with authentic EBOV were performed using Vero E6 cells cultured as previously described (Holtsberg et al., 2015). For rVSV assays Vero cells were used as described (Wong et al., 2010). ADCP was measured using monocyte cell lines THP-1 (human) and RAW264.7 (murine) that were cultured as described (Gunn et al., 2018).

Primary cells

Human NK cells were enriched from human peripheral blood samples using negative selection with RosetteSep (Stem Cell Technologies) followed by Ficoll separation.

Viruses

Mouse-adapted EBOV/Mayinga (EBOV/M.mus-tc/COD/76/Yambuku-Mayinga) was used for neutralization assays involving authentic Ebola virus and for *in vivo* protection studies. EbolaΔVP30-RenLuc virus was used for ΔVP30 neutralization assays and rVSV-EBOV/Mayinga GP (EBOV/H.sap-tc/COD/76/Yambuku-Mayinga) was used for rVSV neutralization assays.

METHOD DETAILS

Expression and Purification of EBOV, Makona variant, BDBV, SUDV, RESTV and Marburg RAVN GPs

Recombinant EBOV GP ectodomain lacking residues 637-676 of the transmembrane domain (GPe) or GP lacking both the transmembrane and mucin domains (residues 312-462; GPeΔmuc) were previously described (Murin et al., 2014). The sGP construct encoded GP truncated at residue P314. All constructs carried a C-terminal double strep tag (enterokinase cleavage site followed by a strep tag/linker/strep tag) for purification and were cloned into modified pMT-puro vectors for expression in *Drosophila* Schneider 2 (S2) cells (Hashiguchi et al., 2015). Stably transfected cells were selected with 6 μg/ml puromycin. The resulting strep-tagged proteins were purified using Strep-Tactin resin (QIAGEN) followed by further purification by SEC using a Superdex 200 (S200) column with 10 mM Tris and 150 mM NaCl, pH 7.5 (1 × TBS). GP_{CL} was produced by incubating 1 mg GPe with

0.02 mg thermolysin overnight at room temperature in TBS with 1 mM CaCl_2 followed by SEC purification on a Superdex 200 SEC column. GPe Δ muc carrying the Q508R mutation was purified as previously described (Murin et al., 2014). RAVV GP (Kenya 1987 Kitum Cave variant) was produced as previously described (Fusco et al., 2015) and BDBV (Uganda 2007 Butalya variant), SUDV (Uganda 2000 Gulu variant) and RESTV (USA 1989 Philippines 89 variant) (Holtsberg et al., 2015) were produced similarly to EBOV. The Makona (West African) ectodomain (GenBank KM034562.1), expressed as per EBOV, has lower trimeric propensity than Mayinga (Central Africa), which could affect mAbs that target quaternary epitopes.

ELISA analysis of antibody binding to GP

ELISA assays were performed as previously described (Murin et al., 2014). Briefly, 96-well plates were coated overnight with the indicated antigen at 0.2 $\mu\text{g}/\text{well}$, washed three times with PBS, and blocked with 3% BSA in PBS for one hour at room temperature. Antibodies were added at 2, 0.2, and 0.02 $\mu\text{g}/\text{ml}$ and incubated for one hour at room temperature. For EC_{50} measurements, 10-fold serial dilutions of antibodies from 20 $\mu\text{g}/\text{ml}$ were measured. After binding, the wells were washed and HRP-conjugated secondary antibody diluted 1:4,000 in 0.5% BSA was added and incubated for 1 hr at room temperature. A TMB substrate kit (Pierce) was used for detection at 450 nm. The reactivity threshold was defined as $\text{OD}_{450} \geq 1.0 \text{ AU}$ at 2 $\mu\text{g}/\text{ml}$ antibody.

Epitope mapping by electron microscopy of IgG Fab fragments complexed with GP Δ TM

Antibody Fabs were prepared as described previously (Bornholdt et al., 2016) and incubated with Zaire GP Δ TM at a ratio of 10:1 (Fab:GP) overnight at 4°C. Complexes were purified by size exclusion chromatography using a Superdex 200 Increase 10/300 GL column (GE Healthcare Life Sciences) before being deposited onto carbon-coated copper mesh grids and staining with 2% uranyl formate. Imaging of the grids using a 120 keV Tecnai Spirit electron microscope and a TemCam F416 4k x 4k CCD was conducted as described (Zhao et al., 2017). Processing of the imaged particles was achieved following organization into stacks and alignment by iterative MRA/MSA, wherein clean 2D particle stacks were subjected to EMAN2 refinement to produce a 3D model, as previously described (Zhao et al., 2017). UCSF Chimera (Pettersen et al., 2004) was used to dock crystal structures of GP Δ TM into the image reconstructions.

Epitope mapping by alanine scanning mutagenesis

Alanine scanning mutagenesis was performed on GP and on GP lacking the mucin-like domain (residues 311–461) wherein residues were mutated to alanine (alanine residues were mutated to serine) to create clone libraries of point mutants. The clones were individually arrayed into 384-well plates and transfected into HEK293T cells and the protein was allowed to express for 22 hr (Davidson et al., 2015). The indicated mAbs were incubated with the cells for 1 hr before an Alexa Fluor 488-conjugated secondary antibody (Jackson ImmunoResearch Laboratories) was added. Antibody binding was assessed by detection of cellular fluorescence with an Intellicyt high throughput flow cytometer (Intellicyt, Albuquerque, NM). Background fluorescence was measured in vector-transfected control cells and mAb reactivity against the mutant clones was calculated with respect to reactivity with wild-type GP Δ TM by subtracting the signal from mock-transfected controls and normalized to signals from wild-type transfected controls. Residues predicted to be involved in the epitope were identified if no reaction was seen between the mAb and the mutant clone, but reactivity of other control mAbs was observed, which excludes GP mutants that are misfolded or had low expression levels.

Neutralization of Ebola Δ VP30-RenLuc virus

An Ebola virus in which the reporter gene *Renilla* luciferase is substituted for the viral transcription factor VP30 (Ebola Δ VP30-RenLuc virus) was used to complement a Vero cell line that stably expresses VP30 in *trans* (Vero VP30), thus allowing analysis at BSL-3 (Halfmann et al., 2008). A total of 5×10^3 focus forming units of Ebola Δ VP30-RenLuc virus diluted in 2% fetal calf serum in minimal essential medium were incubated with 50 $\mu\text{g}/\text{ml}$ monoclonal antibody for 3 hours at 37°C. The virus/antibody mixture at a multiplicity of infection (MOI) of 0.001 was then added to Vero VP30 cells, seeded the previous day in 96-well plates at 9×10^3 cells/well and incubated for three days at 37°C and 5% CO_2 . If used, guinea pig complement (Cedarlane) was added to the minimal essential medium at a final concentration of 10%. Then a live cell luciferase substrate, EnduRen (Promega), was incubated with the cells for three hours before luciferase values were measured as relative light units (RLU) using a Tecan M1000 plate reader (Tecan). Assays were performed in duplicate and a known neutralizing (GP 133/3.16) and non-neutralizing monoclonal (VP35 5/69.3.2) was used as a positive and negative control, respectively. Antibodies that neutralized luciferase signals by $\geq 95\%$ were defined as strong neutralizers, whereas inhibition of luciferase signals by 50%–94% were considered moderate neutralizers and those that had 49% or lower inhibition were categorized as weak/non-neutralizers.

Neutralization of authentic EBOV

Assays to assess neutralization of authentic EBOV were performed according to the method described in Holtsberg et al. (Holtsberg et al., 2015). Vero E6 cells were seeded 2.5×10^{-4} cells/well in the inner 60 wells of black 96-well plates 24 hours prior to virus infection. Antibodies were serially diluted in Vero growth medium (Eagle minimum essential medium with Earle's salts and L-glutamine, 5% fetal bovine serum (FBS) and 1% penicillin-streptomycin) at two times the desired final concentration (50 $\mu\text{g}/\text{ml}$), mixed with an equal volume of live EBOV, and incubated for 1 hour at 37°C with mixing every 15 min. The antibody/virus mixture at a MOI of 0.2 was then added to the Vero cells and incubated for 1 hr at 37°C, washed with PBS, and growth medium alone was added to

all wells and the plates were incubated for an additional 48 hr at 37°C. The cells were then fixed with 10% neutral buffered formalin and the percentage of infected cells was determined by an indirect immunofluorescence assay using the EBOV-specific human mAb KZ52 and goat anti-human IgG conjugated to Alexa Fluor 488 (Molecular Probes) as a secondary antibody. Images were acquired at 20 fields/well with a 20x objective lens on an Operetta High Content Imaging System (Perkin-Elmer). Operetta images were analyzed with a customized algorithm built from image analysis functions available in Harmony software (Perkin-Elmer). The percentage of inhibition for each antibody was determined relative to control cells incubated with media alone. Antibodies that reduced the percentage of infected cells by > 80% were categorized as strong neutralizers, whereas those that reduced infection by between 50% and 79% and less than 50% were considered as moderate neutralizers and weak/non-neutralizers, respectively.

Neutralization of rVSV-EBOV GP

Recombinant vesicular stomatitis virus (VSV) expressing both eGFP and recombinant surface GP (rVSV-EBOV) in place of VSV G was described previously (Wec et al., 2016; Wong et al., 2010). For neutralization assays, Vero cells were seeded at 6.0×10^4 cells/well and cultured overnight in Eagle's minimal essential medium (EMEM) supplemented with 10% fetal bovine serum (FBS) and 100 I.U./ml penicillin and 100 µg/ml streptomycin at 37°C and 5% CO₂. The next day, virus was incubated with serial 3-fold antibody dilutions beginning at 330 nM (~50 µg/ml) in serum-free EMEM for one hour at room temperature before infecting Vero cell monolayers in 96-well plates. The amount of virus used for infection was determined based on titration of viral stock to achieve 35%–50% final infection in control wells without antibody (MOI ~0.1 infectious units per cell). The virus was incubated with the cells in 50% v/v EMEM supplemented with 2% FBS, 100 I.U./ml penicillin and 100 µg/ml streptomycin at 37°C and 5% CO₂ for 14–16 hours before the cells were fixed and the nuclei stained with Hoechst. rVSV infectivity was measured by counting EGFP-positive cells in comparison to the total number of cells indicated by nuclear staining using a Cellinsight CX5 automated microscope and accompanying software (Thermo Scientific). The infection level in control wells lacking antibody was set to 100% and the infection was normalized to that value for each antibody dilution, which were tested in triplicate. The mean value was determined and the full 9-point dilution curve was used to determine the half-maximal inhibitor concentration, IC₅₀ using GraphPad Prism version 6. Antibodies having IC₅₀ ≤ 5 nM were considered strong neutralizers whereas antibodies having 5 nM < IC₅₀ < 50 nM and ≤ 50 nM were considered moderate neutralizers and weak/non-neutralizers, respectively. The un-neutralized fraction, an indicator of antibody potency, was also determined using antibodies at the highest concentration tested, 330 nM, and measuring the GFP signal relative to that of untreated control cells. Those that reduced the signal by ≥ 98%, 50%–98%, and less than 50% were considered strong, moderate, and weak/non-neutralizers, respectively.

Antibody-mediated protection of mice challenged with mouse-adapted EBOV

To gauge antibody protection, a previously described mouse-adapted EBOV mouse model, developed at the U.S. Army Medical Research Institute of Infectious Diseases (USAMRIID) was used (Bray et al., 1998; Gibb et al., 2001). Assays were performed either at USAMRIID or Public Health Agency of Canada (PHAC). Female BALB/c mice, aged 6 to 8 weeks-old (Charles River Laboratory) were housed in microisolator cages and given chow and water *ad libitum*. On day 0 of the assay, the mice were transferred to a biosafety level (BSL) level 4 containment area and challenged intraperitoneally with mouse-adapted EBOV (Mayinga isolate, Yambuku variant, 100 p.f.u. (USAMRIID) or 1,000 x LD₅₀ (PHAC)). On day 2 post-infection, groups of 10 mice were treated intraperitoneally with 100 µg (~5 mg/kg) mAb per mouse. Mice were observed daily for signs of disease and group weights were recorded daily through day 14 and again on days 21 and 28. Mice were observed for at least 21 days after virus exposure, and protection is expressed as the percentage of mice surviving at the end of a 28 day period. For each round of experiments, 0%–20% of mice that received PBS alone survived challenge. All animal work involving infectious live virus was performed in the BSL-4 laboratories at USAMRIID or PHAC. At USAMRIID, all work with animals was conducted in compliance with the Animal Welfare Act and other Federal statutes and regulations relating to animals and experiments involving animals and adhered to the principles stated in the Guide for the Care and Use of Laboratory Animals, NRC Publication, 1996 edition. All procedures were reviewed and approved by the appropriate Institutional Animal Care and Use Committee at USAMRIID. Work performed at PHAC was approved by the Canadian Science Centre for Human and Animal Health Animal Care Committee following the guidelines of the Canadian Council on Animal Care.

Immune effector assays

Antibody mediated cellular phagocytosis by human and mouse monocytes (huADCP and mADCP)

ZEBOV GPΔTM (IBT Biotherapeutics) was biotinylated and conjugated to streptavidin-coated Alexa 488 beads (Life Technologies). The beads were incubated with 5 µg/ml for 2 (huADCP) or 1 (mADCP) hr at 37°C before human (THP-1, 2.5×10^4 cells/well) or mouse (RAW264.7, 1.0×10^5 cells/well) monocytic cells were added and incubated for 18 (huADCP) or 1 (mADCP) hr at 37°C. Following fixation, the cells were analyzed by flow cytometry using a BD LSR2 flow cytometer. Data were analyzed using FlowJo software. A phagocytic score describing relative phagocytic activity was calculated as:

Phagocytic score = (%FITC+ cells x MFI of FITC+ cells)/10,000 where MFI is the mean fluorescence intensity of all FITC+ cells. Each phagocytic score was also compared to that for a non-specific/irrelevant antibody and a control reaction lacking antibody that were both performed in the same experiment to account for cell/donor variability.

Antibody-mediated neutrophil phagocytosis (huADNP and mADNP)

ZEBOV GPΔTM-coated beads as generated for the ADCP assays were incubated with 5 μg/ml mAbs for 2 hours at 37°C before neutrophils isolated from either human peripheral blood or bone marrow from BALB/c mice were added at 5.0×10^4 cells/well or 1.0×10^5 cells/well, respectively, and incubated at 37°C for 1 hour. The cells were then stained for markers of neutrophils (human neutrophils were as defined as high-granularity SSC-A^{high}, CD66b⁺, CD14⁺, CD3⁺; mouse neutrophils were defined as high granularity SSC-A^{high}, Gr-1⁺, CD11b⁺, CD3⁺). Flow cytometry, data analysis and calculation of a phagocytic score were performed as described for the ADCP assays.

Antibody-mediated NK cell degranulation and activation

Human NK cells were enriched from human peripheral blood samples using negative selection with RosetteSep (Stem Cell Technologies) followed by Ficoll separation. Maxisorp ELISA plates were first coated with ZEBOV GPΔTM (3 μg/ml) before blocking with 5% BSA and incubation with 5 μg/ml mAbs at 37°C for 2 hours. The mAbs were removed by washing and NK cells (5.0×10^4 cells/well) in the presence of 10 μg/ml brefeldin A (Sigma Aldrich), GolgiStop (BD), and anti-CD107a were incubated at 37°C for 5 hr. The NK cells were then stained for NK surface markers (CD3, CD56, CD16, BD Biosciences) followed by intracellular staining to detect cytokine and chemokine production (IFN-γ and MIP-1β, BD Biosciences). NK cells were analyzed with a BD LSR2 flow cytometer and data were analyzed using FlowJo software.

Determination of polyfunctionality

Polyfunctionality is scored on a scale of 0–7 that represents the sum of the four phagocytic and three natural killer functions elicited. One point was given for each phagocytic or NK function measured for which the activity was above a defined threshold, which was established using the irrelevant antibody control for Ebola-specific antibody responses, the HIV-specific b12 (PMID: 11498595).

Classification of functional activity into high, moderate, and low

Functional responses were divided into “high,” “moderate,” and “low/none” tritiles based on the responses of the Ebola-specific mAb, c13C6 (PMID: 10698744, 23071322) and the HIV-specific b12. Responses equal or greater to c13C6 were considered “high,” and responses equal or less than b12 were considered “low,” and responses between b12 and c13C6 were considered “moderate.” mAbs that scored medium/high for a given assay were considered functional for that assay.

Analysis of antibody glycan content

A previously described capillary electrophoresis method was used to determine the relative abundance of antibody glycan structures (Mahan et al., 2015). In brief, the Fc region was cleaved from the Fab using the FabRICATOR IdeS (Genovis) and N-linked glycans were removed using peptide-n-glycosidase F (PNGase F, New England BioLabs). The free glycans were then labeled with 50 mM 9-aminopyrene-1,4,6-trisulfonic acid (APTS) in 1.2 M citric acid and 1 M sodium cyanoborohydride in tetrahydrofuran (THF). Excess dye was removed using a size exclusion resin before loading onto a 3130XL Genetic Analyzer (Applied Biosystems) equipped with a 36 cm capillary array with POP-7 polymer. Peaks for 19 substructures were identified and the relative abundance of each structure was determined by calculating the area under the curve for each peak and dividing by the total area of all peaks.

QUANTIFICATION AND STATISTICAL ANALYSES

Machine learning and statistical analyses

The Kruskal–Wallis test was used to identify differences between different epitope classes. Dunn’s test was used to identify pairwise differences. Multiple hypothesis testing was corrected for using false discovery rate. Pairwise Spearman’s ρ calculations and hypothesis testing was done in R. The interactive network at <https://apps.vhfinmunotherapy.org/cornnetwork> to visualize the pairwise Spearman’s ρ coefficients was developed using d3.js (<https://d3js.org/>). The R caret package (<https://cran.r-project.org/package=caret>) was used to build and evaluate machine learning classifiers for the classification task. All features in the dataset were centered and scaled before training the algorithms. As part of data preprocessing, the fusion, GP1/Head and HR2 epitope classes that had near-zero variance were removed from the dataset. The isotype feature was also removed since 100 of the 101 human-derived mAbs were IgG1, which could lead to overestimation of the importance of a certain isotype subset. Values for the unneutralized fraction of rVSV-EBOV were transformed to represent the instantaneous inhibitory potential (IIP). The code used for the analysis and to build the applications used to explore the dataset is hosted at: <https://andersen-lab.github.io/VIC-Analysis/>.

The Python scikit-learn package was used for machine learning predictions of levels of protection conferred by antibodies based on antibody features (Pedregosa et al., 2011). The ExtraTreesRegressor (Geurts et al., 2006) implementation of Random Forest (RF) algorithm (Breiman, 2001) was used for RF regression. Readouts for rVSV-EBOV as well as GPEC₅₀ and sGP EC₅₀ were transformed to Log10 values. RF prediction accuracy was calculated using 10-fold cross-validation.

Supplemental Figures

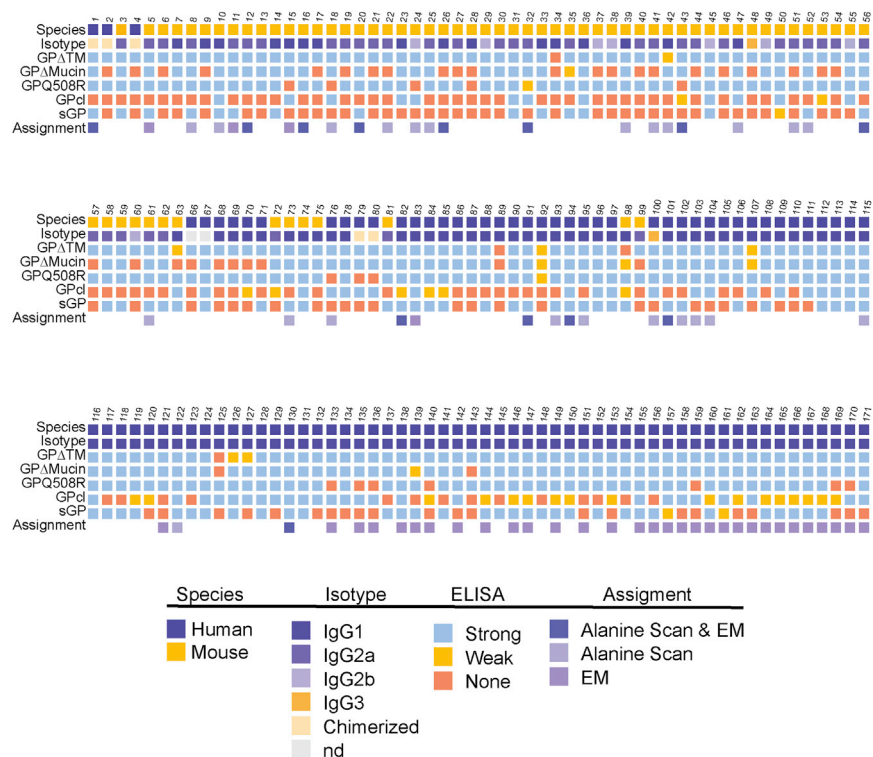


Figure S1. Species, Isotype, ELISA Binding and EM and Alanine-Scanning Assignment of Epitopes, Related to Figure 1

mAb binding to EBOV GP lacking the transmembrane domain or the indicated regions illustrated in Figure 1 was assessed by ELISA and categorized as strong, moderate or weak. Epitopes were confirmed or assigned using ELISA results combined with alanine-scanning and/or electron microscopy results for the indicated antibodies. Isotype nd: not determined.

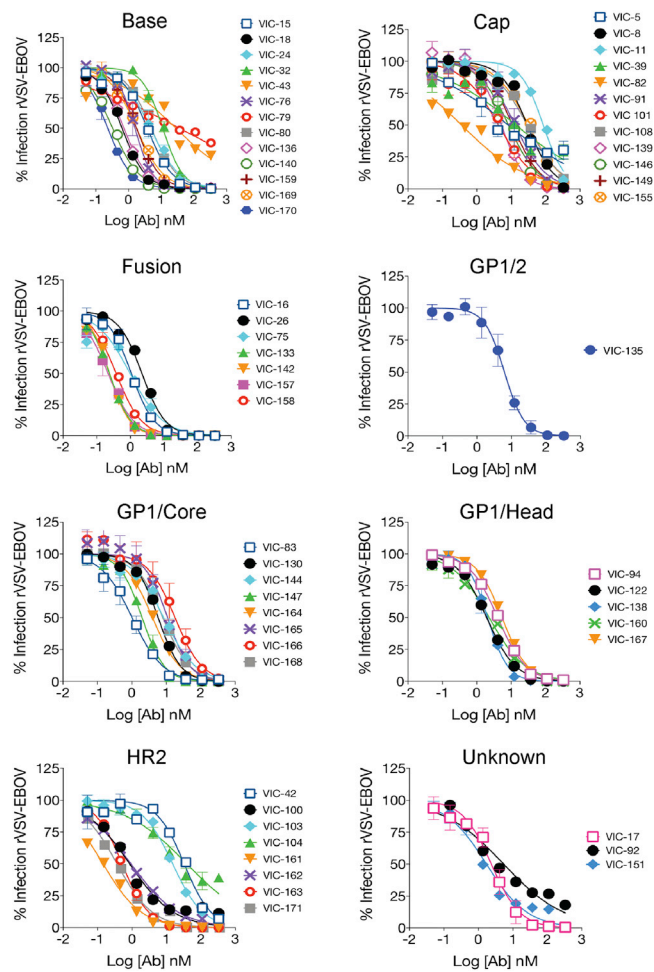


Figure S2. Neutralization of rVSV-EBOV by Epitope Class, Related to Figure 2

Mean \pm SD for three replicates are shown. No mAbs in the mucin class exhibited neutralization activity in this assay and this class is not shown.

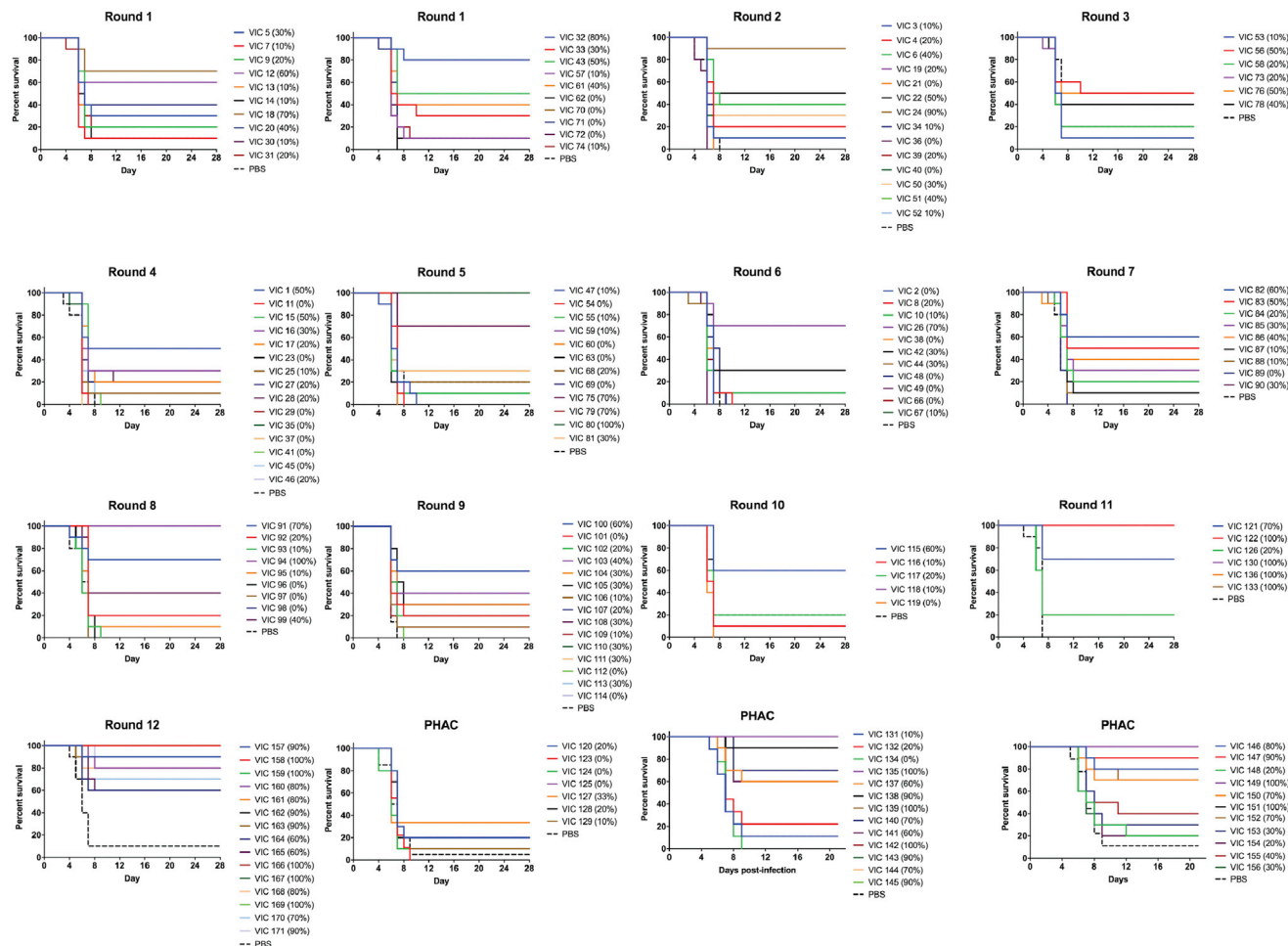


Figure S3. Survival Curves for *in vivo* Protection Assay, Related to Figure 3

mAbs tested at USAMRIID facilities were assayed in 12 rounds. The mice were treated with 100 μ g/ml antibodies on day 2 post-infection and were observed and weighed across a 28 day period. mAbs tested at Public Health Agency of Canada (Manitoba) were tested in one round. The mice were treated with 100 μ g/ml antibodies on day 2 post-infection and observed for a total of 21 days.

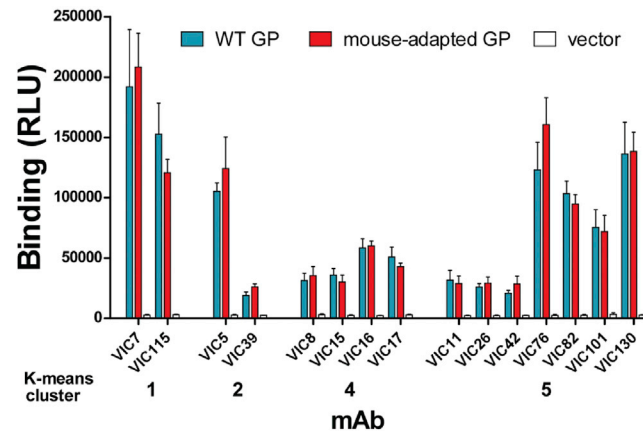


Figure S4. mAb Binding to Wild-Type (WT) and Mouse-Adapted Full-Length EBOV GP, Related to Figure 3

mAbs from K-means cluster groups 1, 2, 4, and 5 (Figure 4) were tested for binding to both WT and mouse adapted EBOV GP. The mAbs included Cluster 1 mAb VIC 115, which protected *in vivo* but did not neutralize. HEK293T cells were transfected with constructs expressing wild-type GP, mouse-adapted GP, or empty vector, and mAb binding was detected by flow cytometry, as described for alanine scanning epitope mapping. Data shown are the average and standard deviation of four measurements of binding, expressed as relative light units (RLU).

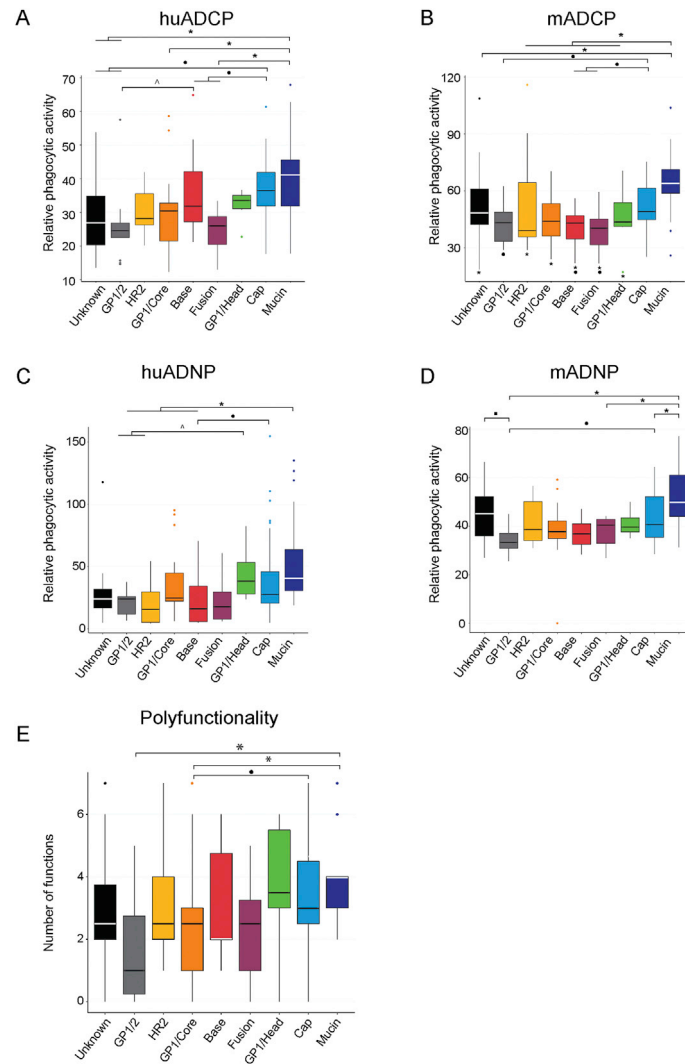


Figure S5. Parametric ANOVA Analysis of Correlations between Epitope Class and Phagocytosis Assay Readouts and Polyfunctionality, Related to Figure 6

Black and white lines indicate mean values. (A) The mean huADCP activity for both mucin and cap was significantly higher than fusion, GP1/2, GP1/Core and unknown (p values ranged from 4.2×10^{-4} –0.039 and 7.9×10^{-4} –0.04, respectively), whereas base was significantly higher than GP1/2 ($p = 0.02$). (B) For mADCP activity, mucin had the highest mean value and was significantly higher than that of all other antibody classes (*p values ranged from 9.3×10^{-4} –0.034), and cap was significantly higher than GP1/Core, GP1/2, fusion and base (●, p values ranged from 0.03 to 0.048). (C, D) The mucin group had the highest mean value for both huADNP and mADNP assays (*p values ranged from 1.2×10^{-4} –0.042) and the other classes in Tier 1, cap (●) and GP1/Head (○) were higher than base ($p = 0.04$) and base, GP1/2 and HR2 (p values ranging from 0.043 to 0.048), respectively. In the mADNP assay, the unknown class had a higher mean value than that for GP1/2 (■ $p = 7.6 \times 10^{-3}$). (E) The mean value for mucin polyfunctionality was significantly higher than that for GP1/2 and GP1/Core antibodies (* $p = 0.0028$ and 0.157, respectively) and the mean value for the Cap class was significantly higher than that for GP1/2 (●, $p = 0.007$).

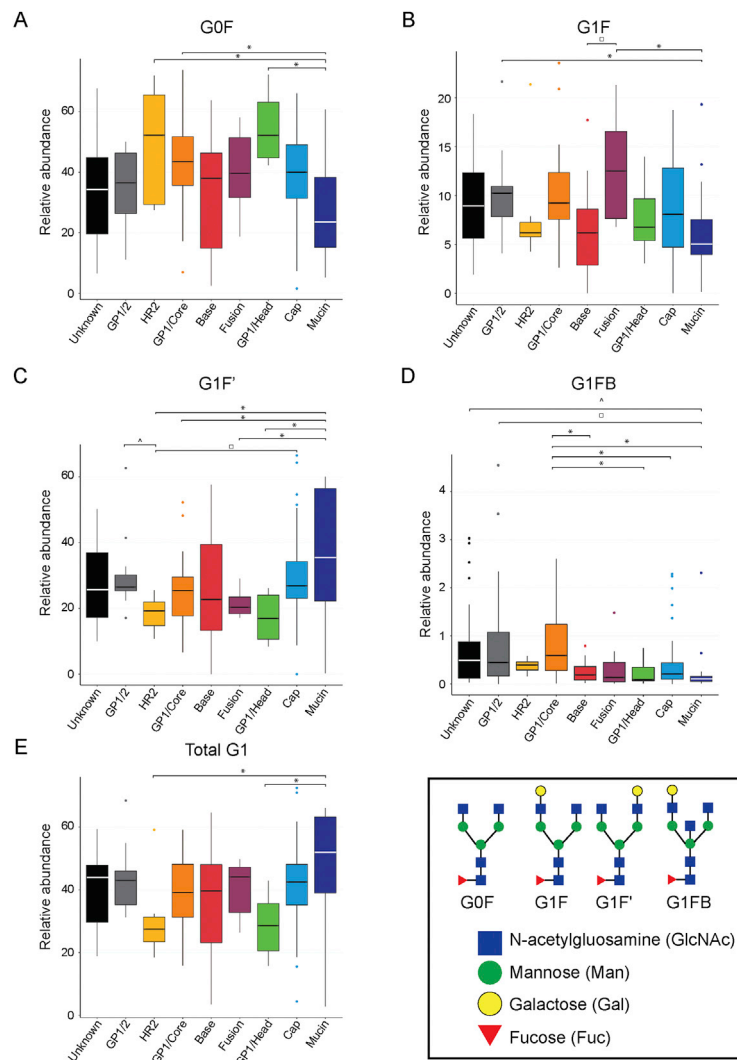


Figure S6. Glycan Modification of VIC Antibodies, Related to Figure 7

The relative abundance of antibody glycan modifications was assessed. Of the 15 species and total amounts of G0, G1, G2, fucose, bisecting GlcNAc, sialic acid and mono-sialic acid, ANOVA identified (A) G0F, (B) G1F, (C) G1F', (D) G1FB and (E) total G0 as having a significant correlation with epitope class. Significant differences are indicated by bars with p values ranging between 4.4×10^{-4} and 0.049.

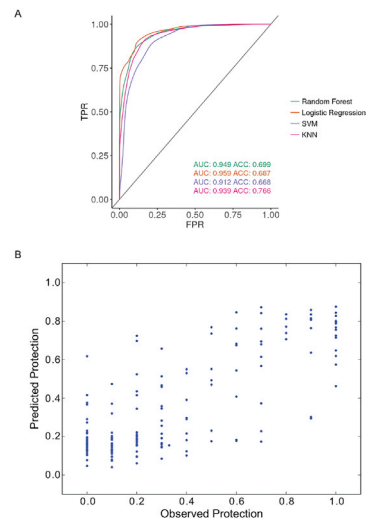


Figure S7. Machine learning algorithms and Random Forest Regression Predictions of Protection, Related to Figure 7

(A) Mean receiver operating characteristic curves of four machine learning algorithms (KNN: K-nearest neighbors; LR: Linear regression; RF: Random Forest; SVM: Support vector machine) trained and tested on dataset, D1, with raw neutralization readouts using a ten-fold cross validation scheme, related to Figure 7. Area under curve (AUC) values are shown in the legend. FPR: False positive rate; TPR: True positive rate. (B) Random forest regression predictions of protection using 10-fold cross validation; all antibody features were used as input for the predictions, related to Figure 7. The mean absolute error was 0.161. The importance factors of the top ten features used for the predictions are shown in Table S4.